**JOURNAL OF FUEL CHEMISTRY AND TECHNOLOGY**
Volume 54, Issue 8, August 2026

燃料化学学报(中英文)
Journal of Fuel Chemistry and Technology

**Cite this article as:** J Fuel Chem Technol, 2026, 54, 20260017

REVIEW

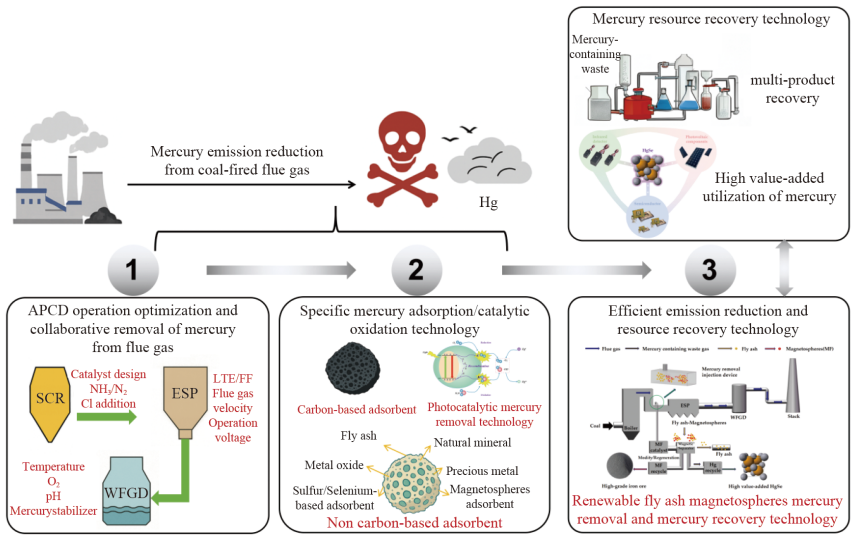
# Control strategy for mercury emissions from coal-fired flue gas in China

**XIAO Rihong, LUO Changxin, WU Yuzi, TANG Chengrui, XIONG Zhuo, ZHANG Junying, ZHAO Yongchun***

State Key Laboratory of Coal Combustion, Huazhong University of Science and Technology, Wuhan 430074, China

**Abstract:** Mercury in the emission from coal combustion is highly toxic, volatile and bioaccumulative, posing a long-term threat to the ecosystems and human health. In this paper, the current status and control policies of mercury emissions from coal combustion in China were systematically reviewed, and the distribution characteristics and transformation mechanisms of mercury during coal combustion were analyzed, with a focus on the mechanisms and performance of collaborative mercury removal in the pollution control devices after ultra-low emission retrofitting. Furthermore, a progressive strategy of "synergistic enhancement-deep purification-resource recycling" for mercury emission reduction was proposed, including three tiers: optimizing the operational parameters of pollution control systems to improve the synergistic mercury removal efficiency of various control devices; developing an efficient mercury adsorption and catalytic oxidation technology for coal-fired flue gas, with a focus on the industrially applicable mercury removal technologies; developing an integrated mercury removal and recovery technology for coal-fired power plants (e.g., magnetospheres mercury removal and mercury recovery technologies), focusing on the high-value utilization of mercury. Finally, combining the latest international compliance requirements and domestic environmental tax policies, the future research directions on the emission control of mercury in coal-fired flue gas in China were outlined, providing theoretical and technical support for the China's international commitments and near-zero emissions of coal combustion pollutants.

**Key words:** coal combustion; mercury; adsorption/catalysis; mercury recovery; emission reduction strategy




*Progressive strategy for mercury emission reduction from coal-fired flue gas*

The proportion of coal in China's primary energy consumption structure has been declining continuously; however, the total national energy consumption increases from 4.28 billion tonnes to 5.72 billion tonnes, and the absolute consumption of coal continues to rise, demonstrating a structural characteristic of "declining the share but increasing total volume". Coal still remains irreplaceable in China's energy system and will continue to serve as the "stabilizing force" in the short term[1]. According to the Coal 2024 report released by the IEA,

Received: 2026-01-14; Revised: 2026-02-02
Foundation items: Supported by National Natural Science Foundation of China (524B2082), Fundamental and Interdisciplinary Disciplines Breakthrough Plan of the Ministry of Education of China (JYB2025XDXM302).
* Corresponding author. Tel: 13419608698, E-mail: yczhao@hust.edu.cn.
DOI: 10.1016/S1872-5813(26)60708-6 CSTR: 32157.14.2097-213X.2026.JFCT.0068
本文的英文电子版由 Elsevier 出版社在 ScienceDirect 上出版 (http://www.sciencedirect.com/science/journal/18725813)

China's coal consumption accounts for approximately 56% of the global total, with the power sector being the largest consumer[2]. Developing efficient and economical pollutant control technologies for coal-fired power plants is of great strategic significance and urgency for promoting the modernization of China's environmental governance system.

Mercury (Hg) is widely recognized as one of the most hazardous pollutants due to its pronounced toxicity, volatility, mobility, and bioaccumulation. Once the atmospheric mercury enters water bodies and soils through natural deposition, it can be transformed into more toxic methylmercury under microbial action. This organomercury compound can accumulate progressively along the ecological food chains and eventually enter the human body, leading to damage to the central nervous system and potential dysfunction of organs such as kidneys and liver. The atmospheric mercury emission sources can be categorized into natural and anthropogenic sources. Natural sources primarily include volcanic eruptions, forest fires, and soil erosion processes, whereas anthropogenic sources mainly encompass industrial activities such as coal combustion, iron and steel smelting, and cement production. According to the Global Mercury Assessment 2018 published by the United Nations Environment Programme (UNEP), human activities have become a significant source of atmospheric mercury, with annual emissions reaching approximately 2500 tonnes, accounting for 56.81% of the global total emissions[3]. As a major coal-consuming country, developing efficient and low-cost mercury pollution control technologies in China holds an important practical significance and a strategic value for the protection of ecological environment.

The international community has reached broad consensus on mercury pollution issues. The Minamata Convention on Mercury, promulgated by the United Nations Environment Programme, aims to promote the global mercury emission reduction and governance. As one of the first contracting parties, China has actively responded and formulated the strategies for mercury pollution prevention and control. In 2011, China issued the standards of emission limit for mercury and its compounds from coal-fired power plants, stipulating that the mercury concentration in flue gas should not exceed 30 μg/m$^3$. However, compared with developed countries, there is still a certain gap in the limit value. For instance, the United States has implemented more stringent emission standards for non-lignite coal-fired power plants, in which the mercury emission from new units should not exceed 0.39 μg/m$^3$, while for the existing units it should not exceed 1.7 μg/m$^3$. The European Union, in turn, adopts a tiered management approach based on the unit capacity, with the limit values of 1−3 μg/m$^3$ for the new units of <300 MW and 1−2 μg/m$^3$ for the new units of ⩾300 MW[4]. Therefore, as one of the largest global mercury emitters, China's coal-fired power plant emission limits are bound to continue tightening. On January 1, 2018, the Environmental Protection Tax Law of the People's Republic of China came into effect, imposing environmental taxes on the top three pollutants in coal-fired power plant emissions. The pollution equivalent value of mercury in atmospheric pollutants is 0.0001 kg. According to calculations, coal-fired power plants are now subject to a mercury tax, as the pollution equivalent value of their mercury emissions has surpassed that of soot emissions. For example, a 1000 MW coal-fired unit emits nearly 100 kg of mercury annually, corresponding to a pollution equivalent value of 1000000, and with a tax rate ranging from 1.2 to 12 CNY per equivalent value (varying by province), mercury emissions have become a significant expenditure item for coal-fired power plants' environmental protection taxes[5]. In November 2025, the Sixth Meeting of the Conference of the Parties to the Minamata Convention on Mercury (COP6) further reviewed and strengthened the implementation progress of Parties in reducing mercury supply and controlling unintentional emissions, such as those from industrial releases and waste treatment[6]. Therefore, the control of mercury emissions from coal-fired power plants has become an urgent issue.

During coal combustion, mercury is primarily released into the flue gas in gaseous phase and exists in three forms: particulate-bound mercury ($Hg^p$), oxidized mercury ($Hg^{2+}$), and elemental mercury ($Hg^0$). With the full implementation of ultra-low emission retrofit projects in China's coal-fired power plants, the pollution control systems of traditional coal-fired units have shifted from single pollutant control devices (such as desulfurization, denitrification, and dust removal) to multi-pollutant synergistic control systems. However, without the retrofit, the mercury removal efficiency by the single pollutant control device was generally low. For instance, the Selective Catalytic Reduction (SCR) system typically used honeycomb or plate-type catalysts arranged in a "2+1" configuration, with only one layer of catalyst left as a backup, resulting in a higher gas velocity within the SCR reactor, shortening the contact time between $Hg^0$ in the flue gas and the catalyst, and making it less conducive to the oxidation of $Hg^0$. In addition, coal-fired units generally used traditional high-temperature dust removal systems to remove $Hg^p$. Because the $Hg^p$ concentration in the flue gas is relatively low and the particle size mainly ranges from 0.1 to 1.0 μm, so the capture efficiency by the traditional dust removal devices (electrostatic precipitators) is limited, with a removal rate usually below 30%[7]. Although the limestone-gypsum wet flue gas desulfurization (WFGD) technology, as a typical flue gas desulfurization process, can achieve a removal rate of over 85% for $Hg^{2+}$, due to the stable chemical properties of $Hg^0$ and its insolubility in water, the synergistic removal efficiency in the WFGD system is very limited[8]. In summary, in light of the current situation where the mercury emission control efficiency in the existing coal-fired units in China is low, to reach the more stringent future mercury emission limits, there is an urgent need to develop efficient mercury reduction technologies and synergistic control strategies that are suitable for China's coal-fired units.

Based on an systematic analysis of China's mercury emission control needs and technological development trends in coal combustion, this review advanced a three-tiered progressive mercury reduction strategy suitable for coal-fired units. First, in the context of ultra-low emission retrofits, the distribution characteristics of mercury in the coal-fired flue gas treatment process were outlined, the mechanisms and influencing factors of pollution control systems, such as SCR, ESP and WFGD, in the synergistic removal of mercury were analyzed. Second, in response to the low efficiency of mercury synergistic control in the existing coal-fired units, a technical approach to improve the collaborative mercury removal performance of the control devices by adjusting operating parameters and optimizing system configurations was suggested. Next, the recent advances in the mercury adsorption and catalytic oxidation technologies for coal-fired flue gas and the current field applications of mercury removal technologies in the China's coal-fired flue gas treatment were summarized. Then, the progress in the mercury resource recovery and high-value utilization technologies for the multiphase by-products during mercury removal in the coal-fired power plants was discussed. Finally, in light of the international compliance requirements and domestic environmental policy trends, the future development directions of mercury reduction and resource utilization technologies in the China's coal-fired power plants were looked ahead to, aiming to provide a systematic theoretical basis and technical support for achieving mercury control and near-zero emissions for coal-fired flue gases.

## 1 Distribution, migration and transformation of mercury during the coal combustion process

The mercury content and its occurrence forms in coal directly influence the release and control strategies of mercury during coal combustion. Zhang et al.[9] indicated that a calculated arithmetic mean of mercury based on over 900 coal samples from China was 0.158 μg/g. Finkelman et al.[10] discovered that mercury in coal was mainly associated with the sulfide minerals such as cinnabar, pyrite, galena, and sphalerite. Additionally, mercury in coal may also exist in the forms of metallic mercury, organic mercury, mercuric chloride, and selenides. For the specific occurrence forms of mercury in coal, Liu et al.[11] confirmed that mercury was mainly present in the sulfide-bound and residual forms, based on the continuous leaching experiments. Liu et al.[12] did a combustion experiment using a one-dimensional furnace at 1200 °C, compared the mercury content in raw coal and fly ash, and found that more than 85% of mercury volatilized in the gas phase, with less than 6% remaining in the bottom ash. Zheng et al.[13] tested the mercury emissions from a 300 MW coal-fired unit using the Ontario-Hydro method, which indicated that mercury completely volatilized during combustion and remained mainly in the gas phase even at the dust removal temperatures, with weak condensation phenomena. Approximately 86% of mercury was found in the flue gas, 13% in the particulate mercury in fly ash, and only about 1% in the bottom slag. As shown in Figure 1, mercury in the flue gas mainly existed in three forms: $Hg^0$, $Hg^{2+}$ and $Hg^p$.

The migration and transformation of mercury can be summarized as follows: after coal particles underwent pyrolysis and ignition, a large amount of volatile matter was released, and the carbonaceous particles continued to burn and fragment into smaller particles[14]. In the high-temperature flame, almost all mercury in coal was converted to elemental mercury ($Hg^0$)[15−16]. With the decrease of flue gas temperature, $Hg^0$ reacted with halogens ($Cl_2$, $Br_2$), acidic gases (HCl, HBr, $NO_2$) and $O_2$ in the flue gas to generate $Hg^{2+}$[17−18].

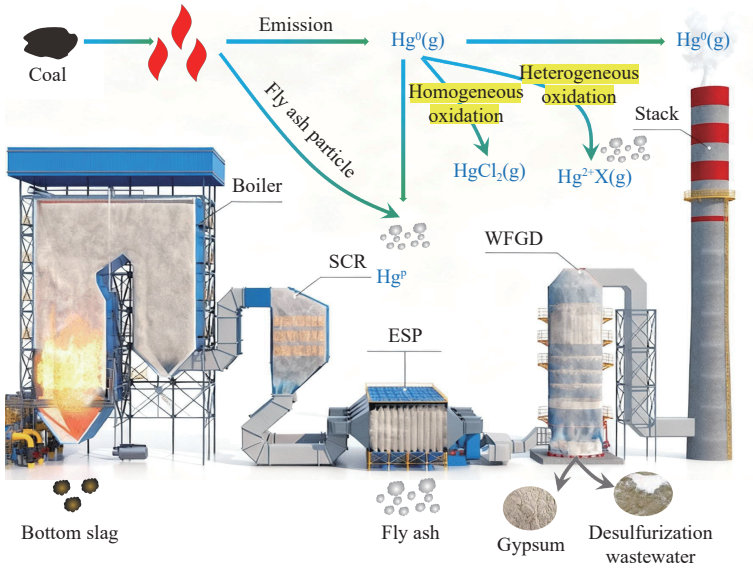



Fig. 1 Pollution control device in the coal-fired power plant and distribution of mercury migration and transformation during coal combustion

Part of $Hg^{2+}$ could further adsorb onto the fly ash surface. Simultaneously, under the catalysis of fly ash surface and flue gas components, part of the $Hg^0$ could form particulate $Hg^p$ through heterogeneous oxidation and adsorption[19]. In addition, some $Hg^0$ still flew out with the flue gas in the gas phase. In summary, $Hg^{2+}$ in the flue gas was easily soluble in water and attached to the particulate matter, $Hg^p$ could be collected by the dust removal equipment, while $Hg^0$ was volatile, difficult to dissolve in water, and difficult to capture, thus almost all of it was released into the atmosphere.

## 2 Current status of collaborative mercury removal control in ultra-low emission retrofit

The existing flue gas purification devices in coal-fired power plants (Air Pollution Control Devices, APCD) have a certain synergistic effect on the mercury removal, but the removal efficiency largely depends on the occurrence forms of mercury in the flue gas. The main pollutant control devices in coal-fired power plants include Selective Catalytic Reduction (SCR), particulate removal devices (Electrostatic Precipitators, ESP and Fabric Filters, FF), and Wet Flue Gas Desulfurization (WFGD). Therefore, the key to achieving mercury emission reduction for coal-fired flue gas is to clarify the synergistic removal effects of different pollutant control devices on various forms of mercury ($Hg^0$, $Hg^{2+}$ and $Hg^p$), and accordingly to carry out the targeted process optimization and improvement.

### 2.1 SCR denitration system

The SCR system typically operates at around 350 °C, where $NH_3$ is used to reduce $NO_x$, producing $N_2$ and $H_2O$[20−21]. In addition to its denitrification function, the SCR catalyst also has a certain catalytic oxidation effect on $Hg^0$[22]. As shown in Figure 2(a), after SCR treatment, the concentration of $Hg^0$ significantly decreased, while the concentration of $Hg^{2+}$ increased, indicating that the core role of SCR was to promote the oxidation transformation of $Hg^0$, and this oxidation capability remained relatively stable during long-term operation[23]. Preciado et al.[24] found that HCl was adsorbed and dissociated on the $V_2O_5$-$TiO_2$ catalyst surface, forming active intermediate complexes that promoted the $Hg^0$ oxidation reaction. Additionally, Figure 2(b) shows that higher ammonia-to-nitrogen ratio ($NH_3/N_2$) had an inhibitory effect on the oxidation of $Hg^0$, because the strong adsorption of $NH_3$ occupied the active sites on the catalyst surface, reducing the adsorption of HCl and thereby decreasing the oxidation efficiency. Moreover, Zhou et al.[25] found that when the boiler load increased from 60% to 100%, the flue gas residence time was shortened, and the oxidation efficiency of $Hg^0$ decreased from 72.10% to 61.78%. Although SCR can effectively regulate the form of mercury, especially by oxidizing to reduce the $Hg^0$ concentration, the direct contribution to total mercury removal is limited. Future studies should focus on optimizing the process parameters, particularly the factors such as ammonia-to-nitrogen ratio and chlorine content, to further improve the oxidation efficiency of $Hg^0$, thereby enhancing the mercury removal effectiveness of SCR.

### 2.2 ESP dust removal system

As the flue gas temperature gradually decreased after passing through the heat exchange surfaces, a portion of the gaseous mercury can be adsorbed onto the surface of fly ash and subsequently transformed into particulate-bound mercury ($Hg^p$)[26]. Field measurements conducted by Fthenakis et al.[27] demonstrated that ESPs achieved the mercury removal efficiencies of 20%−26%. The studies by Zhang et al.[28−30] showed that in contrast to conventional ESPs, the low-temperature electrostatic precipitators (LTEs) exhibited significantly superior performance in the particulate-bound mercury removal.

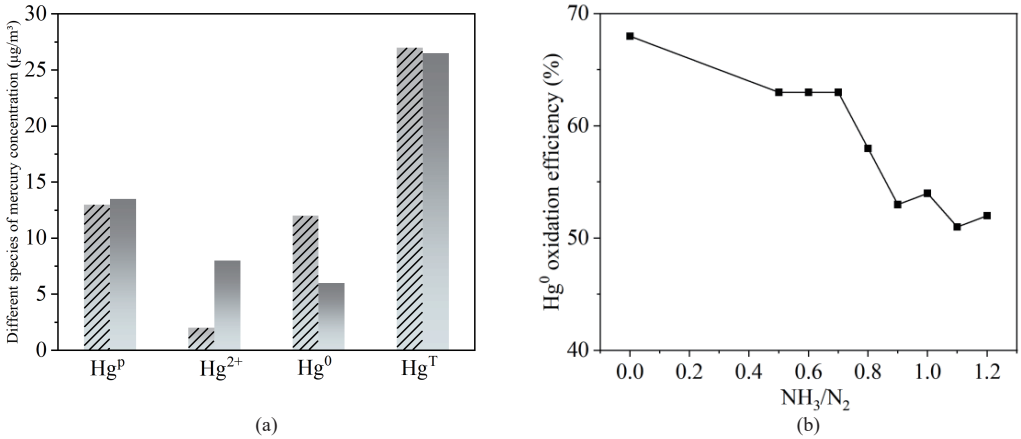



Fig. 2 (a) Changes in various mercury species and total mercury before and after SCR[23] and (b) relationship between ammonia to nitrogen ratio and $Hg^0$ oxidation rate[25]
(with permission from ACS Publications)

As illustrated in Figure 3, the reduction in temperature facilitated the enhanced adsorption of both elemental mercury ($Hg^0$) and oxidized mercury ($Hg^{2+}$) onto the fly ash surfaces, thereby improving the capture efficiency of $Hg^p$. Fabric filters (FFs) were demonstrated to have better performance than ESPs in terms of synergistic mercury removal, primarily attributed to their effective capture of submicron particles (0.1−1 μm)[31]. The properties of coal also influenced the synergistic mercury removal performance of ESPs. The mercury removal efficiency for the bituminous coal fired and coal/petroleum coke co-fired units was 35%−54%, while the mercury removal efficiency for the subbituminous coal and lignite fired units was relatively low, which were mainly attributed to the variations in chlorine content and mercury speciation distribution in different coal types[32]. Although ESP systems have shown certain advantages in capturing particulate mercury, they still have some limitations. ESPs exhibit relatively low collection efficiencies for submicron particles (0.1−1 μm), and their effectiveness in removing gaseous $Hg^0$ is limited. Furthermore, the mercury removal efficiency of ESPs is largely dependent on the operational parameters such as flue gas temperature, flow gas velocity and fly ash characteristics, rendering the removal performance susceptible to the variations in operating conditions. The future research aimed at enhancing the ESP mercury removal performance should focus on two key aspects: first, intensifying the investigations on the influencing factors such as fly ash particle size distribution and coal properties, coupled with improvements in the design of precipitator and the optimization of operating conditions; second, integrating novel sorbent technologies or catalysts to augment the capability of ESP systems in removing gaseous $Hg^0$.

### 2.3 WFGD desulfurization system

WFGD is one of the most critical units for synergistic mercury removal in the coal-fired power plants, owing to the high solubility of $Hg^{2+}$ in the slurry[33−35]. As illustrated in Figure 4, the testing results from Li et al.[36] revealed that $Hg^{2+}$ underwent a reduction reaction within the WFGD system and was subsequently re-emitted in the form of $Hg^0$. VanLoon et al.[37] analyzed in detail the primary mechanisms for the reduction process: (1) The water film reaction mechanism: A thin water film was formed through the evaporation of lime or limestone slurry, within which $Hg^{2+}$ reacted with $Hg^0$ to generate $Hg_2^{2+}$ and the $Hg_2^{2+}$ subsequently reacted with $OH^-$ in the slurry to produce $Hg^0$ and HgO, with the latter being further reduced to $Hg^0$ by $SO_2$; (2) The solution reaction mechanism: $SO_2$ from the flue gas was dissolved into the slurry to form sulfite and sulfate species, which then reacted with $Hg^{2+}$ to produce $HgSO_3$ and $HgSO_4$. A portion of the resulting mercury compounds was chemically unstable and consequently decomposes, resulting in the re-emission of elemental mercury ($Hg^0$). Additionally, Li[38] observed that elevating temperature accelerated the ion migration rates, thereby enhancing the reduction reactions, whereas increasing the pH of slurry inhibited the mercury re-emission due to the formation of stable $Hg(OH)^+$ and $Hg(OH)_2$ complexes. Conversely, increasing $O_2$ concentration in the flue gas reduced the pH of slurry, thereby promoting the $Hg^0$ emission.

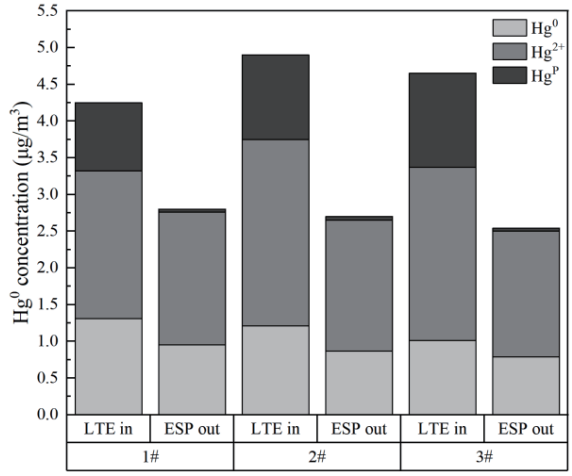



Fig. 3 The influence of cold electrostatic precipitators on the distribution of different forms of mercury in flue gas under different units[31]
(with permission from Elsevier)

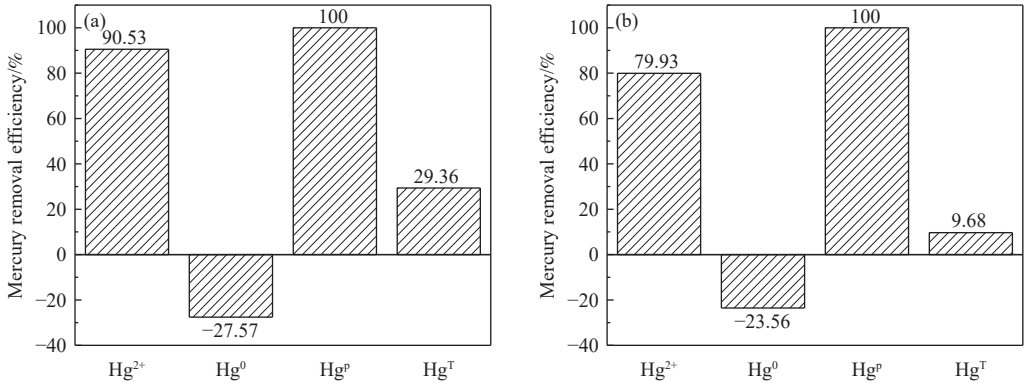



Fig. 4 The removal efficiency of WFGD for different forms of mercury ($Hg^{2+}$, $Hg^0$, $Hg^p$) under different operating conditions[36]
(with permission from Elsevier)

The aforementioned studies demonstrate that although the WFGD systems exhibit remarkable removal efficiency for $Hg^{2+}$, their removal efficiency for $Hg^0$ is relatively low, and there is an issue of $Hg^{2+}$ reduction and subsequent re-release. To enhance the comprehensive mercury removal performance of WFGD systems, future research should focus on optimizing the operational conditions, such as adjusting the pH of slurry and temperature, to minimize the $Hg^0$ re-emission, and exploring the integration with other mercury control technologies to improve the overall system performance.

## 3 Collaborative mercury removal with multi pollutant control devices based on operation optimization

The preceding section systematically analyzed the synergistic mercury removal performance of the existing flue gas purification devices in the coal-fired power plants. The results indicate that different pollutant control units exhibit distinct selectivity and complementarity in mercury removal. Specifically, SCR for denitrification primarily oxidizes a portion of $Hg^0$ to $Hg^{2+}$ but cannot effectively reduce the total mercury concentration in flue gas; ESP is only effective for the removal of $Hg^p$, with limited removal efficiency for $Hg^0$; and WFGD mainly targets the removal of $Hg^{2+}$, with the mercury removal efficiency being dependent on the proportion of $Hg^{2+}$ in the flue gas. Therefore, relying on a single device or fixed operating conditions makes it difficult to achieve desired mercury removal performance. Without modifying the existing desulfurization, denitrification, and particulate removal systems, enhancing the synergistic effects among purification units by optimizing the operating parameters and conditions to improve mercury transformation and capture efficiency is the first-tier mercury reduction strategy. This strategy focuses on improving the overall mercury removal performance of existing systems by making full use of the characteristics and advantages of each device, thereby facilitating the effective mercury control.

### 3.1 Optimization of SCR system operation and collaborative mercury removal

During the SCR synergistic mercury removal process, achieving optimal synergy between denitrification and mercury removal requires adjustments across three dimensions: fuel optimization, operational optimization, and catalyst optimization. (1) Fuel optimization: The chlorine content in coal exerts a significant influence on the mercury speciation transformation. Elevating HCl concentrations facilitates the conversion of chlorine into highly oxidative free radical Cl or $Cl_2$, thereby promoting the oxidation of $Hg^0$[39]. However, coal-fired power plants in China predominantly utilize low-chlorine coals, resulting in relatively low catalytic conversion efficiency of mercury in the SCR systems. This limitation can be addressed *via* the supplementation of HCl or the co-firing of high- and low-chlorine coals to enhance the mercury removal efficiency, but attention should be paid to avoiding increased equipment corrosion and operational costs. Therefore, it is necessary to balance the mercury removal efficiency with economic feasibility, with the goal of ensuring the long-term stable operation of the system. (2) $NH_3$/NO ratio optimization: Under the conditions using low-chlorine coal, the competitive adsorption occurs between $NH_3$ and HCl, which inhibits the oxidation of HCl on $Hg^0$ and consequently reduces the synergistic mercury removal efficiency of SCR. To enhance the SCR performance, experimental investigations and online monitoring should be employed to optimize the $NH_3$/NO ratio, thereby minimizing the ammonia slip while maintaining high mercury removal efficiency. (3) Denitrification catalyst optimization: The denitrification and mercury removal performance of SCR systems are contingent upon the catalyst activity and composition. Modified catalysts can further improve the mercury removal efficiency. As illustrated in Figure 5, Zhao et al.[40] modified the spent $TiO_2$-based SCR catalysts with Ce-Mn oxides for $Hg^0$ removal, achieving an $Hg^0$ oxidation rate as high as 92.80%. Nevertheless, the high cost and the stability of such catalysts are of significant challenges. Future research should focus on optimizing the cost-effectiveness of catalysts, exploring the inexpensive yet highly efficient materials, and ensuring the long-term stability under high-pollution conditions.

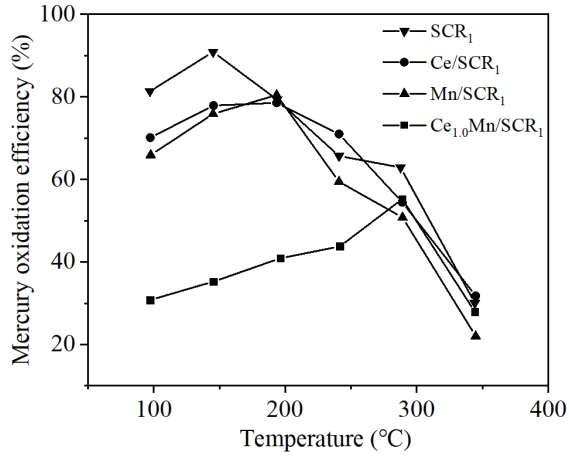



Fig. 5 $Hg^0$ oxidation efficiency over different catalysts under simulated flue gas as a function of temperature[40]
(with permission from Elsevier)

### 3.2 Optimization of ESP system operation and collaborative mercury removal

By improving the dust removal efficiency of the ESP system, the particulate concentration in the flue gas can be

reduced, thereby enhancing the capture efficiency of both $Hg^p$ and $Hg^{2+}$. The optimization strategies include two approaches: one is to change the type of dust collector, such as replacing the ESP with a low-temperature electrostatic precipitator (LTE), adopting fabric filters (FFs), or adding a wet electrostatic precipitator (WESP) behind the ESP. The other is to optimize the operating parameters of the electrostatic precipitator, adjusting the flue gas flow velocity and the working voltage to improve the mercury removal efficiency. Li[41] demonstrated that under sorbent injection conditions, a reduced flue gas velocity increased the contact time between sorbents and mercury in the flue gas, thereby improving the removal efficiency. Conversely, an elevated flue gas velocity shortened the residence times and thereby diminished the removal performance. Furthermore, the relationship between working voltage and mercury removal performance did not exhibit a linear positive correlation. At lower voltages, the particles are under charged, while at higher voltages, the particle residence time is shortened, thereby affecting the adsorption process. Consequently, the selection of an appropriate flue gas velocity and a working voltage is a critical factor for enhancing the mercury removal efficiency. Future research should focus on exploring how to balance gas velocity, particulate removal efficiency, and mercury removal efficiency, especially in different types of units. At the same time, an intelligent control system should be introduced to achieve more precise process optimization and improve the overall mercury removal efficiency.

### 3.3 Optimization of WFGD system operation and collaborative mercury removal

Due to high water solubility of $Hg^{2+}$, the $Hg^{2+}$ generated through oxidation in SCR units can be absorbed by the desulfurization slurry in WFGD systems. However, the reduction and re-emission of $Hg^0$ in the desulfurization systems constrain the overall mercury removal efficiency. To address this problem, researchers have proposed two primary solutions: (1) introducing oxidizing agents into the WFGD tower to oxidize $Hg^0$ into absorbable $Hg^{2+}$; and (2) adding mercury-stabilizing agents to the desulfurization slurry to facilitate the reaction of oxidized mercury with sulfur to form stable precipitates, thereby suppressing the $Hg^0$ re-emission. Fang et al.[42] demonstrated that the addition of potassium permanganate ($KMnO_4$) effectively promoted the $Hg^0$ oxidation, with the mercury removal efficiency progressively increasing with $KMnO_4$ concentration and ultimately reaching 100%. Omine et al.[43] conducted a comparative investigation with various additives, including sodium hydrosulfide (NaHS), sodium sulfide ($Na_2S$), TMT-15, and Nalco-8034. The results indicated that these additives could substantially immobilize the $Hg^{2+}$ under specific reaction conditions, achieving the removal efficiencies of 99%, 97.1%, 93.2% and 98.9%, respectively. Additionally, as illustrated in Figure 6, Wu et al.[44] found that the addition of sodium tetrasulfide ($Na_2S_4$) effectively inhibited the $Hg^0$ re-emission, with an optimal dosage of 0.00125%. The underlying mechanism involved the decomposition of $Na_2S_4$ into sulfide ions ($S^{2-}$) and elemental sulfur under weakly acidic conditions, which subsequently reacted with $Hg^{2+}$ to form stable mercury sulfide (HgS) precipitates, thereby effectively immobilizing the mercury. The studies by Tang et al.[45] and Ochoa-Gonzalez et al.[46] further confirmed that other additives, such as $Na_2S$, TMT, and DTCR, were equally effective in suppressing the $Hg^0$ re-emission and promoting the migration of $Hg^{2+}$ to the solid phase. Although these methods effectively inhibit the $Hg^0$ re-emission, the precise control of the dosage of additives is required in practical applications to avoid additional costs. Current researches are mostly conducted in the laboratory, and in the future, the practical application effects and economic feasibility should be verified through pilot and full-scale tests.

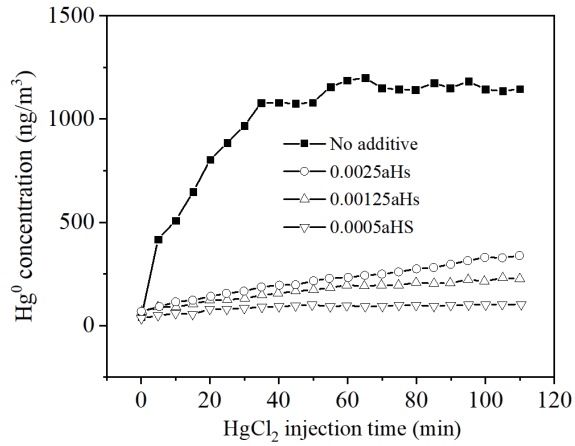



Fig. 6 The effect of sodium thiosulfate ($Na_2S_4$) on suppressing zero mercury emissions[44]
(with permission from Elsevier)

## 4 Development of mercury deep purification (adsorption/catalytic oxidation) technology for coal-fired flue gas

Although the synergistic mercury removal can be achieved to a certain extent through the optimization of operating conditions and structural modifications of the existing pollutant control devices (SCR, ESP, WFGD), the sole reliance on these systems is insufficient for stable, continuous, and efficient mercury removal with various coal-fired units. Due to the differences in furnace configurations, coal types, flue gas compositions, and operating conditions between different power plants, there are significant fluctuations in the synergistic mercury removal effect, especially when using low chlorine coal or when the active components in the flue gas are insufficient, the efficiency of mercury oxidation by SCR and the mercury absorption by WFGD will significantly decrease. In addition, the synergistic effects of some systems are

limited by their primary functions (e.g., desulfurization or particulate removal), resulting in limited direct removal capability for $Hg^0$. Therefore, to further enhance the mercury removal efficiency for coal-fired flue gas, researchers have begun to focus on actively promoting the adsorption and oxidation of $Hg^0$ through the external addition of sorbents or catalysts, advancing the industrial demonstration and application of the technologies. This technical approach is regarded as the secondary mercury reduction strategy. Compared with the strategies relying exclusively on the synergistic mercury removal, this approach offers more stable and efficient mercury removal performance under diverse operating conditions.

### 4.1 Research and development of mercury removal adsorbent for flue gas

#### 4.1.1 Carbon based adsorbent

Carbon-based sorbents have been extensively employed in the flue gas mercury removal due to their large specific surface areas and excellent adsorption characteristics. The mechanism of mercury removal primarily involves the capture of mercury by physical adsorption or chemical reactions. This technology has achieved mature application in industrial processes such as coal-fired power plants and is regarded as one of the efficient approaches for mercury emission control[47]. Activated carbon injection (ACI) is one of the most mature and widely applied adsorption technologies in the field of flue gas mercury removal in the coal-fired power plants[48−49]. However, the performance of activated carbon is substantially influenced by operating conditions and flue gas composition; specifically, the mercury removal efficiency decreases significantly when the flue gas temperatures exceed 150°C[50]. Furthermore, $SO_2$/$SO_3$ and $H_2O$ in the flue gas have marked inhibitory effects on the mercury removal[51−52]. Additionally, the fine particle size of activated carbon powder results in low capture efficiency by ESPs, leading to the potential entrainment by flue gas and the subsequent greenhouse effect[53]. From an economic perspective, although activated carbon can achieve a mercury removal rate of approximately 82%, the mercury removal cost ranges from 693 to 945 CNY/g, greatly exceeding the 164 CNY/g mentioned in the UNEP reports[54]. When the ACI technology is operated in conjunction with the fabric filter systems, an annualized operating cost increases to approximately 51.03 CNY/kW (calculated at an exchange rate of 6.3 against US dollar)[55]. The research by Ancora et al.[56] further indicated that for a 600 MW coal-fired unit, the initial capital investment for the ACI technology is approximately 10 CNY/kW, with an annual operating cost of 11 CNY/kW; when coupled with the fabric filters, the cost would rise to approximate 20 CNY/kW/year. Despite significant improvements in the mercury removal efficiency, the substantial operating expenses still constrain the economic feasibility of this technology.

#### 4.1.2 Research and development of non carbon based adsorbents/catalysts

Given the numerous drawbacks associated with the scaled application of activated carbon powder in the coal-fired power plants in China due to the inherent physicochemical properties, researchers have explored various non-carbon-based adsorbent materials[57−58], including natural minerals, metal oxides, precious metals, fly ash, and calcium-based compounds. These materials have significant advantages in the adsorption efficiency, process adaptability, and thermal stability, which can better meet the practical needs of mercury emission control in the coal-fired power plants in China.

(1) Fly ash

Fly ash, as a major byproduct of coal-fired power plants, has the advantages of high output, wide availability, and low cost, and is therefore considered a promising adsorbent material[59−60]. Fly ash contains unburned carbon and various metal oxides, with the potential of mercury removal from coal combustion flue gas by adsorption and catalytic oxidation. The mercury removal performance of fly ash is influenced by the factors including particle size, pore structure, surface functional groups, and the type and distribution of transition metal oxides[61−62]. Although the fly ash possesses certain mercury adsorption capacity, its overall removal efficiency is relatively low and a typical chemical modification is needed. The research by Zhang et al.[63] demonstrated that a brominated fly ash can significantly improve the mercury removal effectiveness, with the performance primarily dependent on the modification process conditions and the brominating agent type.

(2) Natural mineral adsorbents

Recent studies have indicated that natural minerals have favorable physicochemical adsorption properties for gaseous mercury[64]. Common natural mineral materials include zeolite, diatomite and palygorskite. Untreated minerals are relatively weak in removing gaseous $Hg^0$, and usually need to be modified by chemical or physical means to improve their mercury removal ability[65]. Cai et al.[66] employed KI and KBr for the surface modification of natural clay; when 3% KI was introduced into the clay, the $Hg^0$ removal rates of 78%−89% were achieved after 3 h of adsorption in a $N_2$+$O_2$ mixed atmosphere. Shen et al.[67] prepared a titanium-pillared clay (Ti-PILC) impregnated with KI. Compared with the original clay, this new material had a higher specific surface area and a rich 2−10 nm mesoporous structure, and its $Hg^0$ removal ability was significantly improved. Furthermore, as illustrated in Figure 7, Liu et al.[68] loaded various active species including $CuCl_2$ onto the palygorskite (Pal) surfaces and evaluated the mercury removal performance under simulated flue gas conditions.

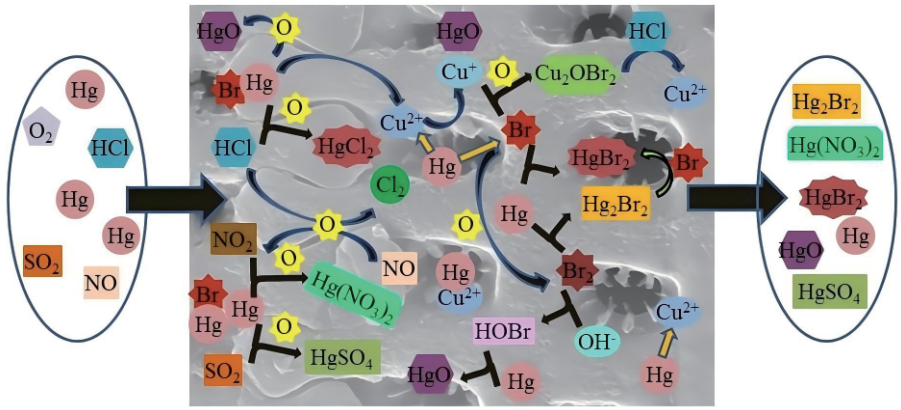



Fig. 7 The removal mechanism of $Hg^0$ by $CuBr_2$-Dia2 in simulated flue gas atmosphere[68]
(with permission from Elsevier)

The results demonstrated that the mercury removal efficiency of the modified adsorbent was significantly improved. The mercury removal rates of $CuCl_2$ Pal and $CuBr_2$ Pal were 90.9% and 95.2%, respectively, while the mercury removal rates of the other modified materials exceeded 80%. Oxygen and hydrogen chloride were confirmed to promote the mercury removal reactions, whereas $SO_2$ and $NO_x$ exhibited the inhibitory effects.

(3) Metal oxide

Metal oxides are considered a promising adsorbent material due to their relatively low cost and strong environmental adaptability[69−70]. The lattice oxygen within the structures can effectively promote the mercury oxidation reactions, exerting a positive catalytic effect[71]. Manganese-based oxide catalysts are extensively employed for the low-temperature $Hg^0$ oxidation and NO reduction, owing to their prominent redox characteristics[72], favorable thermal stability, and relatively low preparation costs[73−74]. However, a single-component manganese oxide suffers from deactivation, particle agglomeration, and insufficient electrical conductivity during operation; therefore, it is commonly combined with other oxides such as Ti and Ce to enhance the performance. Dong et al.[75] prepared manganese-doped Ti-Zr and Ti-Sn composite metal oxides *via* co-precipitation methods. Experimental results showed that at a reaction temperature of 200 °C, the mercury removal efficiencies with these two materials reached 95.4% and 99.3%, respectively. As illustrated in Figure 8, $CeO_2$ is a low-cost rare earth oxide with high catalytic activity and excellent oxygen storage capacity[76]. At low temperatures, $CeO_2$ catalysts can effectively promote the $Hg^0$ oxidation, attributed to the increased reactivity brought about by oxygen vacancies in its lattice. Density functional theory (DFT) calculations have indicated that $CeO_2$ nanorods exhibit superior catalytic activity due to exposure of the specific crystal facets and abundant active sites[77].

(4) Precious metal adsorbents

Precious metal-modified adsorbent materials typically utilize noble metals such as palladium (Pd) and silver (Ag) as the active components[78]. Owing to their excellent thermal stability and regenerability under high-temperature conditions, precious metals have been extensively applied for the mercury capture from flue gas[79]. Due to its strong chemical inertness, high thermal and electrical conductivity, and excellent recyclability, silver has attracted considerable attention for cyclic adsorption-regeneration applications and is regarded as a reusable and highly efficient adsorbent material[80]. Xie et al.[81] investigated the mercury removal performance of silver-loaded SBA-15 and found that when the silver nanoparticles were deposited onto SBA-15, mercury removal efficiencies exceeding 90% could be achieved at 150 °C, attributable to the formation of silver amalgam between mercury and silver nanoparticles. Luo et al.[82] examined the mercury removal performance of carbon nanotubes (CNTs) and silver-loaded carbon nanotubes (Ag-CNTs). The results indicated that the adsorption performance of Ag-CNTs was substantially enhanced after loading silver nanoparticles; even at 150 °C, Ag-CNTs maintained exceptionally a high mercury capture capacity. Consequently, Ag-CNTs were suitable for the mercury removal from coal-fired flue gas, as illustrated in Figure 9. In contrast, Pd exhibited a higher enthalpy of amalgamation, lower material consumption per unit, and a longer regeneration lifespan. Pd-loaded adsorbents were therefore recognized as representative precious metal adsorbents[83].

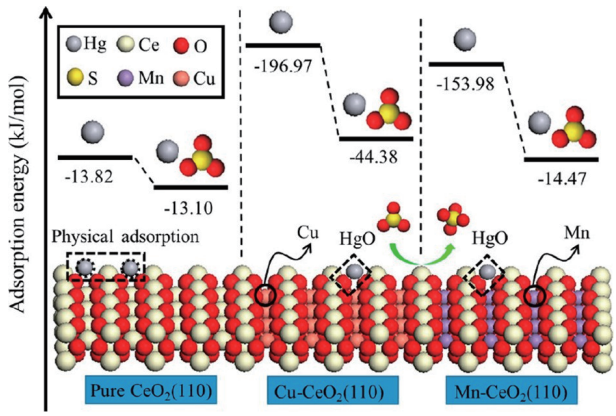



Fig. 8 Adsorption of mercury on copper/manganese doped $CeO_2$ (110) surface[76]
(with permission from ACS Publications)

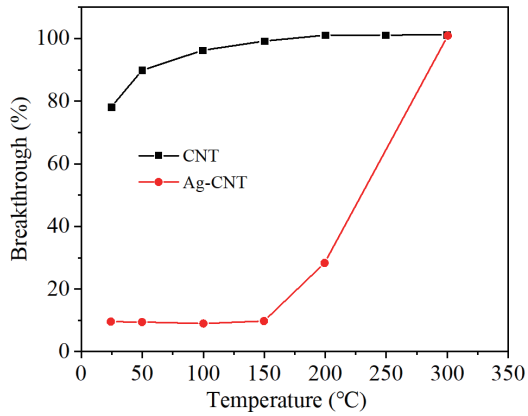



Fig. 9 Mercury removal test of CNT and Ag-CNT[82]
(with permission from ACS Publications)

(5) Sulfur-based adsorbents

Metal sulfides possess superior $Hg^0$ adsorption capacity compared to conventional adsorbents due to their structures containing abundant unsaturated sulfur sites. Liu et al.[84] investigated the mercury removal performance of metal sulfide adsorbents (CuS, MnS, SnS, ZnS and CdS) in simulated flue gas with a high mercury concentration (1300 μg/m$^3$). Among these, CuS showed the most promising results, achieving nearly 70% of mercury removal efficiency after 3 h of reaction at 50 °C, along with good resistance to $SO_2$. Xiao et al.[85] conducted the mercury removal experiments, revealing that $MoS_2$ exhibited the strongest $Hg^0$ removal capability, with a minimal influence from varying adsorption temperatures, gas compositions ($O_2$, NO, $SO_2$), and other reaction conditions (Figure 10). Owing to its abundant edge unsaturated sulfur sites, $MoS_2$ demonstrated excellent resistance to sulfur and outstanding long-term stability, achieving an equilibrium adsorption capacity of 54.308 mg/g and an initial adsorption rate of 66.79 μg/(g·min), which was superior to most metal sulfide adsorbents.

(6) Selenium-based adsorbents

Metal selenides exhibit distinctive chemical reaction characteristics during mercury removal. The selenium vacancies on their surface can strongly coordinate with $Hg^0$, promoting the redox reactions and forming stable Se-Hg covalent bonds, ultimately generating chemically bonded HgSe nanocrystals. Since most metal selenides contain $Se^{2-}$, the relatively low binding energy makes $Se^{2-}$ more prone to react with Hg than the Se–Se bonds in elemental selenium[86]. As illustrated in Figure 11, Xiao et al.[87] reported the synthesis of a novel three-dimensional hierarchical flower-like $SnSe_2$ material and its first application for the mercury capture from flue gas. Under the influence of low-coordination selenium, the introduction of numerous selenium vacancy defects led to exposure of the additional active sites within the adsorbent. The presence of Sn enhanced the gas selectivity and promoted the electron transfer processes, thereby strengthening the $Hg^0$ adsorption and oxidation performance. To further enhance the flue gas mercury adsorption capacity of adsorbents, Li et al.[88] proposed a biomimetic approach to adsorb $Hg^0$ onto the surface of sulfur-rich polyphenylene sulfide (PPS), and utilize Se active sites to migrate weakly adsorbed mercury to the Se sites for permanent fixation. Long et al.[89] synthesized a highly active amorphous red nano-selenium *via* liquid-phase reduction for the efficient mercury adsorption at ambient temperature, and proposed a purification process of mercury selenide (HgSe). However, this approach is unsuitable for the high-temperature industrial flue gas systems, because it may result in decreased adsorbent activity. Consequently, amorphous elemental selenium is not applicable for the high-temperature mercury removal as confirmed by the experimental data of Wang et al.[90]

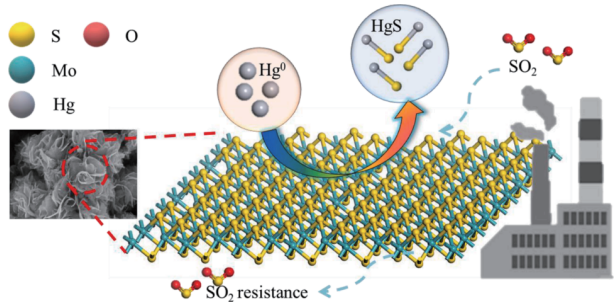



Fig. 10 Adsorption mechanism of $MoS_2$ on elemental mercury in flue gas[85]
(with permission from Elsevier)

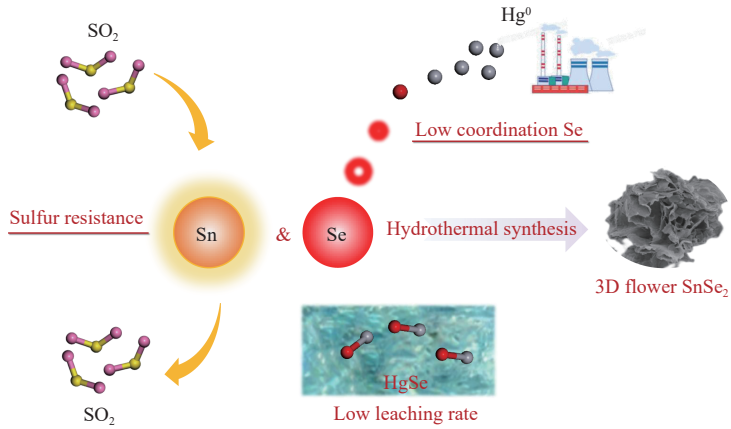



Fig. 11 Adsorption mechanism of $SnSe_2$ on elemental mercury in flue gas[87]
(with permission from ACS Publications)

(7) Regenerable magnetospheres adsorbents

Magnetospheres are a solid byproduct of fly ash from coal-fired power plants[91], mainly composed of iron oxides and possessing certain capabilities for mercury oxidation and adsorption[92]. By virtue of the magnetic characteristics, the magnetic beads adsorbed with mercury can be efficiently separated from fly ash by magnetic separation, so as to realize the recycling. Zhang et al.[91] first proposed a novel concept using magnetic beads for the mercury removal. Figure 12 illustrates the technical principle of mercury removal technology with recycled modified magnetospheres. Firstly, the magnetic separator is used to efficiently separate the magnetic beads from fly ash, and the adsorbed mercury is separated by thermal desorption, with the desorbed gas entering a mercury recovery unit for elemental mercury extraction, while the treated magnetic beads are regenerated by heating. Subsequently, the mercury-removed magnetospheres were sent to a modification device to reconstruct stable, highly active adsorption sites on their surfaces; and the modified magnetospheres are injected into the upstream of flue gas before the electrostatic precipitator (ESP) to remove $Hg^0$ via oxidation and adsorption. The spent magnetospheres enter a magnetospheres separating device again for screening, and finally the efficient recycling of magnetospheres is realized. The mercury removal and recovery system using magnetospheres is composed of magnetospheres separation devices, magnetospheres regeneration and mercury recovery devices, and magnetospheres modification and injection devices.

In 2023, the production of fly ash in China reached approximately 827 million tonnes[93]. The magnetic beads content in fly ash from different sources varies considerably, generally ranging from 0.5% to 18.1%[94]. Based on this estimation, approximately 6.2 million tonnes of magnetic beads could be produced annually in China, indicating the enormous potential as a mercury removal adsorbent with outstanding cost competitiveness. Compared with conventional adsorbents, magnetospheres have the advantages of low cost, recyclability, and easy separation[95]. The iron content in magnetospheres typically ranges from 27.4% to 50.4%, with a primary constituent of $Fe_3O_4$, γ-$Fe_2O_3$, α-$Fe_2O_3$ and silicate glass phases containing $Fe^{2+}$ and $Fe^{3+}$; and the proportion of iron phases varies in the magnetic beads from different power plants. Among them, $Fe_3O_4$ and γ-$Fe_2O_3$ are the key magnetic components[96], accounting for 54.5%−82.9% of the iron-containing substances. Studies have demonstrated that, apart from reaction temperature, the iron content of magnetic beads is a critical factor influencing the mercury removal performance[97]. Yang et al.[98] conducted the mercury removal performance tests with magnetic beads from multiple power plants in the temperature range of 100−400 °C, with the results indicating an optimal $Hg^0$ removal capability at 250 °C. Compared with the coal in the United States, the coal in China has markedly lower chlorine content (63−318 mg/kg), substantially below the average level of American coal (approximately 628 mg/kg)[99]. Furthermore, China possesses abundant coal reserves, and the combustion environments are complex, which makes it particularly important to develop an oxidant that can efficiently remove mercury even under conditions of no or low HCl concentration. Yang et al.[100] modified the magnetospheres with $CuCl_2$ using the equal volume impregnation method, resulting in an increase in mercury removal efficiency to 90.6%. The optimal performance of adsorbent was achieved at a $CuCl_2$ loading of 6% and a reaction temperature of 150 °C. This adsorbent exhibited a minimal influence on the $SO_2$ and NO activity in the flue gas, with good resistance to $SO_2$ and $H_2O$ poisoning[101−102]. The mechanism of the interaction between $CuCl_2$ on the modified magnetic beads surfaces and $Hg^0$ is illustrated in Figure 13.

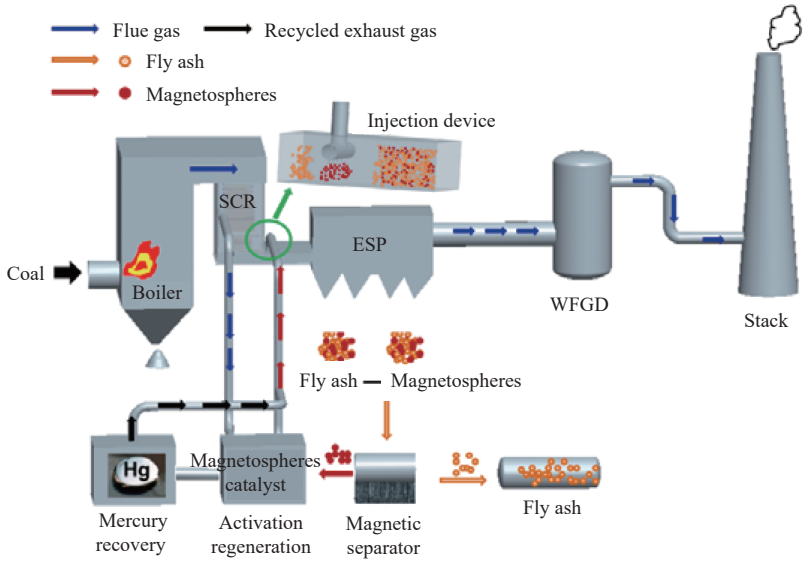



Fig. 12 Schematic diagram of mercury removal and mercury recovery system with magnetospheres[91] (with permission from Elsevier)

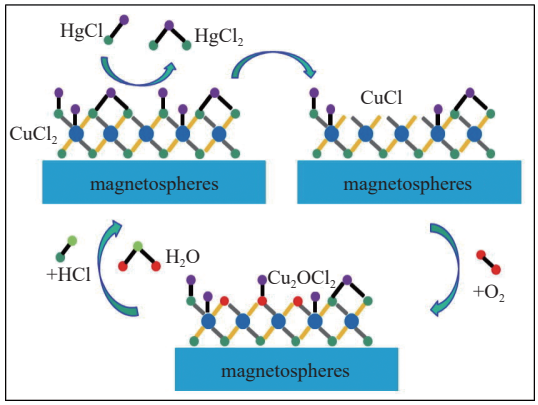



Fig. 13 The mechanism of $CuCl_2$ and $Hg^0$ on the surface of modified magnetospheres[101]
(with permission from Elsevier)

Under conditions of the coexistence of $O_2$ and HCl, $CuCl_2$-modified magnetic beads exhibited excellent regenerability. This was attributable to that $O_2$ facilitated the conversion of $Cu^+$ to $Cu^{2+}$, thereby accelerating the catalytic oxidation of $Hg^0$; simultaneously, HCl compensated for the chlorine consumption during $HgCl_2$ formation, stabilizing the mercury conversion to $Hg^{2+}$ speciation.

### 4.2 Catalytic oxidation mercury removal technology

Among numerous photocatalytic mercury removal materials, $TiO_2$ is the most extensively applied representative catalyst[103−104], which has been widely studied and applied due to its excellent chemical stability, low cost, non-toxicity, and outstanding photocatalytic activity[105]. However, the electron-hole pairs generated by $TiO_2$ under illumination conditions rapidly recombine in a very short period of time, significantly limiting its photocatalytic efficiency. To address this limitation and enhance the mercury removal capability, researchers have proposed various modification strategies. Among them, cerium oxide ($CeO_2$) has outstanding optical and catalytic performance due to its reversible redox properties of $Ce^{3+}/Ce^{4+}$ thereby garnering widespread attention in the photocatalytic mercury removal research[106]. In addition, bismuth-based photocatalysts are a class of visible light catalysts with promising applications, which have a narrow bandgap, strong internal electric field, and much higher photocatalytic performance than common nanocatalysts. As illustrated in Figure 14, Zhang et al.[107] pioneered the development of modified bismuth-based catalysts and their first application in visible-light photocatalytic mercury removal, wherein iodine-doped bismuth tungstate catalytic materials achieved an increase in elemental mercury removal efficiency from 9.1% to 87.6% under visible light irradiation.

In summary, the advantages and limitations of the existing mercury emission control technologies are presented in Table 1. For instance, although activated carbon-based adsorbents demonstrate the relatively stable mercury removal performance, the higher preparation and operating costs and the sensitivity to the variations in the flue gas composition result in limited engineering adaptability.

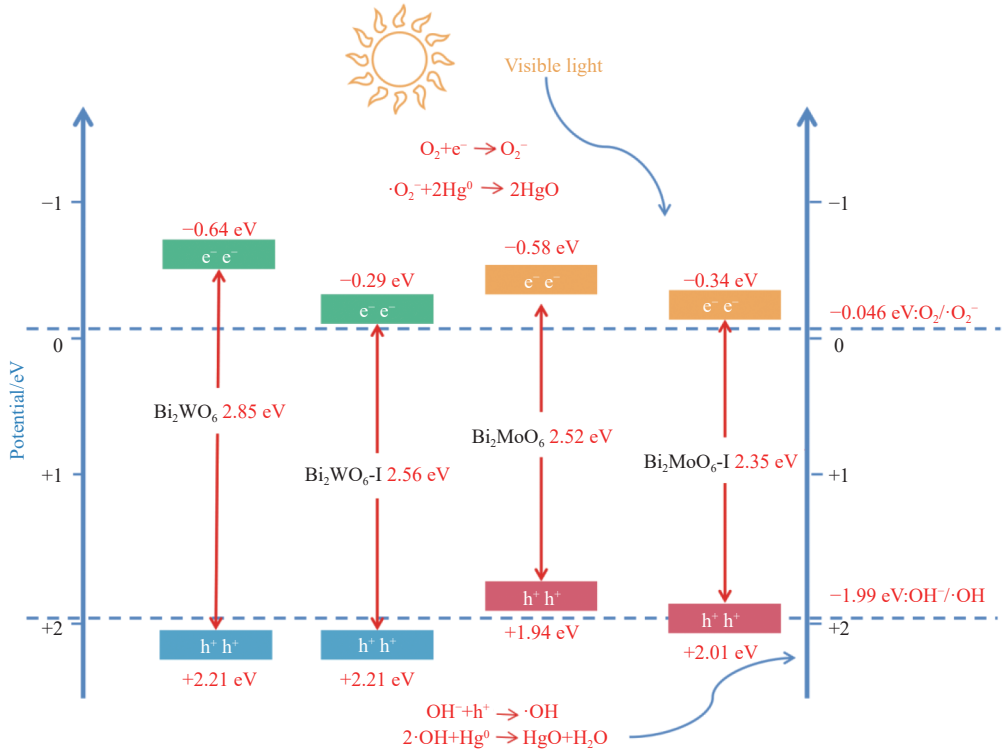



Fig. 14 Visible light photocatalytic mercury removal mechanism of I-doped $Bi_2WO_6$ photocatalyst[107]
(with permission from Elsevier)

Table 1 Advantages and disadvantages of existing mercury emission control technologies

| Mercury emission control technology | Category | Advantages | Disadvantages |
|---|---|---|---|
| Adsorbent injection flue gas mercury removal technology | Activated carbon | Technology is mature and commercially used | High operating costs, with risk of secondary mercury release, and increased burden on dust collector equipment |
| | Biomass-derived carbon | Low raw material cost | Low adsorption capacity, and poor regeneration performance |
| | Fly ash | Low price and wide range of sources | The mercury removal efficiency is significantly influenced by its physicochemical properties |
| | Natural mineral adsorbents | Low price, abundant reserves, and strong adsorption capacity | Many impurities and complex composition |
| | Metal oxide | Abundant oxygen active sites and good mercury removal performance | Poor resistance to $SO_2$ |
| | Precious metal adsorbents | High mercury removal efficiency and strong resistance to flue gas components | High cost |
| | Sulfur-based adsorbents | Excellent sulfur resistance and water tolerance | Narrow operating temperature range |
| | Selenium-based adsorbents | Selenium and mercury have a strong binding force, and HgSe exhibits extremely high stability | Insufficient adsorption rate |
| | Regenerable magnetic beads adsorbents | Low cost, highly efficient and recyclable | The particle size of magnetic beads is small, needing high-precision separating equipment |
| Photocatalytic oxidation mercury removal technology | | Efficient mercury oxidation, environmentally friendly | Strong dependence on light source, poor adaptability to flue gas |

In contrast, non-carbon-based adsorbents have alleviated the application challenges faced by carbon-based materials to some extent; however, these adsorbents usually have complex synthesis processes, high costs, and stringent application conditions, currently remaining only in the experimental research stage. Catalytic mercury removal technologies face the significant challenges including strong dependence on the light sources and poor flue gas adaptability, making the industrial-scale application difficult. Magnetic beads adsorbents use the magnetic components in fly ash to efficiently remove mercury with a regeneration and cyclic operation, having great potential for application. Consequently, given the harsh conditions such as high flue gas volume, low pollutant concentration, and large dust loads in power plants, the development of economically efficient mercury removal technologies is an important direction for future development.

## 4.3 Demonstration and application of flue gas mercury removal technology

This subsection presents some non-carbon-based adsorbent technologies for the coal-fired flue gas mercury removal that have been demonstrated in domestic power generation units. Relevant studies have identified the optimal operating parameters for these adsorbents through field trials, providing important references for the future commercial demonstration of mercury removal technologies. Additionally, a comprehensive evaluation of the advantages and disadvantages of the aforementioned technologies is provided.

### 4.3.1 Mineral adsorbent jet mercury removal

Liu et al.[108] evaluated the mercury removal performance of modified mineral adsorbents ($CuBr_2$-modified coal-bearing claystone partings, designated $CuBr_2$-TCS) in a demonstration project at a domestic 50 MW power plant (Figure 15)[108], and investigated the effects of injection rate and particle size on the mercury distribution in various solid and liquid emission products. The results showed that when $CuBr_2$-TCS was injected at 67.4 kg/h with a particle size of 300 mesh, the relative removal efficiency of total mercury ($Hg^T$) in flue gas at the WFGD outlet reached 82.9%, indicating $CuBr_2$-TCS with promising industrial application prospects. Additionally, higher injection rates and smaller particle sizes of $CuBr_2$-TCS resulted in an elevated mercury concentration in fly ash.

### 4.3.2 Fly ash adsorbent injection mercury removal

Zhang et al.[109] employed an industrial byproduct fly ash as the adsorbent substrate at a domestic 300 MW coal-fired unit, modified the fly ash mechanically and chemically with

bromide to have a high surface energy, and injected the fresh modified fly ash with active sites into the flue for mercury adsorption (Figure 16). By the injection and adsorption of modified fly ash or activated carbon (AC) adsorbents, the mercury concentrations at the ESP outlet decreased from 3.5 to 0.8 μg/m$^3$. This demonstration indicated that modified fly ash was comparable in performance to ACI, and the fresh surface with higher surface energy had a positive influence on adsorption.

#### 4.3.3 Renewable magnetospheres adsorbent jetting mercury removal

Yang et al.[110] conducted the magnetospheres injection experiments in simulated flue gas experimental apparatus, systematically investigating the effects of injection rate and residence time on the mercury removal efficiency, and determining the critical parameters such as optimal particle size and residence time for the magnetospheres injection. To validate the mercury removal performance of modified magnetospheres adsorbents in actual flue gas, Zhou et al.[111] performed the flue gas mercury removal tests using low-cost, recyclable $CuCl_2$-modified magnetospheres (Cu-MF) in a 50 MW coal-fired unit. Field trials demonstrated that with the magnetic beads injection, the mercury concentration at the stack outlet decreased to 0.10 μg/m$^3$, with an overall mercury removal rate of 99.3%. As illustrated in Figure 17, Xiao et al.[112] further validated the mercury removal effectiveness of modified magnetospheres in a 1000 MW unit, the largest capacity coal-fired unit domestically, achieving a flue gas mercury removal rate of 98.72%, with a final flue gas mercury emission concentration of 0.334 μg/m$^3$ and a mercury recovery rate of 52.76% from flue gas. The modified magnetospheres were injected into coal-fired flue gas *via* pneumatic conveying; and the uniform dispersion of particles in the flue gas was a critical factor determining the mercury removal efficiency. Xiao et al.[113] developed a single-hole swirl injector comprising a swirling module (with the key structures such as swirling vanes, swirling sleeve, and swirling diffuser), which enhanced the magnetospheres dispersion in the turbulent flue gas through air swirling, thereby significantly improving the adsorbent coverage and residence time across the flue gas cross-section. The results demonstrated that compared with conventional straight-nozzle lances, the swirl injector improved the mercury removal efficiency by approximately 41.3%, reaching 88.7%. Mercury was highly enriched on the surface of spent magnetic beads during mercury removal.

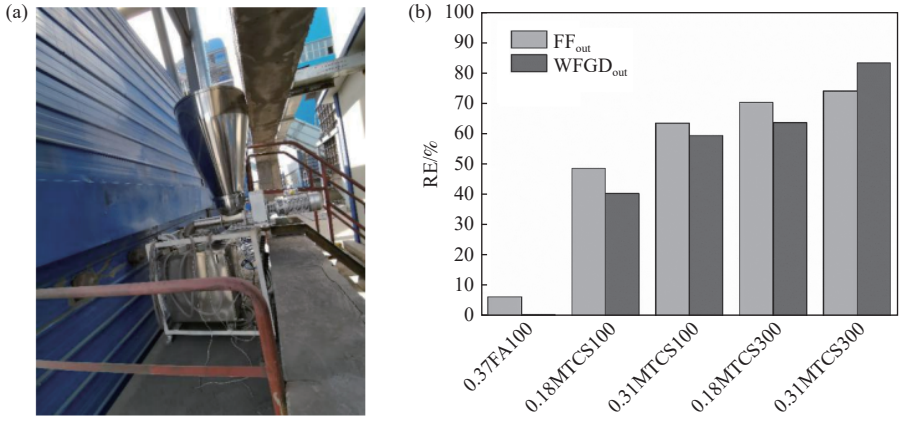



Fig. 15 Injection mercury removal test of modified mineral adsorbent: (a) Injection device diagram, (b) mercury removal efficiency from flue gas after adsorbent injection[108]
(with permission from Elsevier)

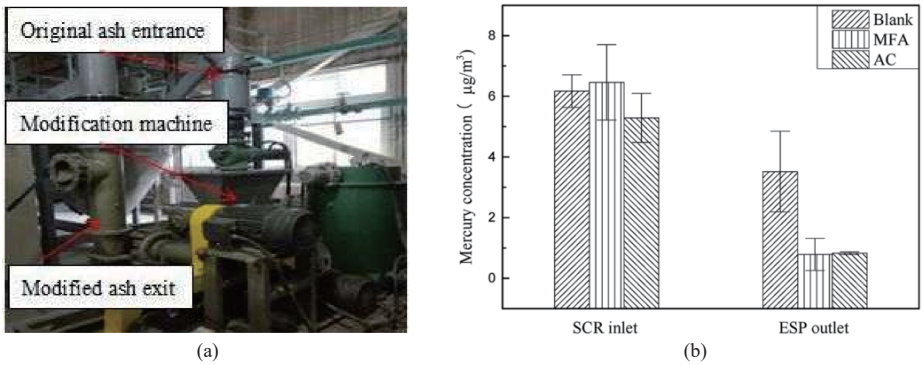



Fig. 16 Injection mercury removal test of modified fly ash adsorbent: (a) Injection device diagram, (b) mercury concentration at different locations after adsorbent injection[109]
(with permission from ACS Publications)

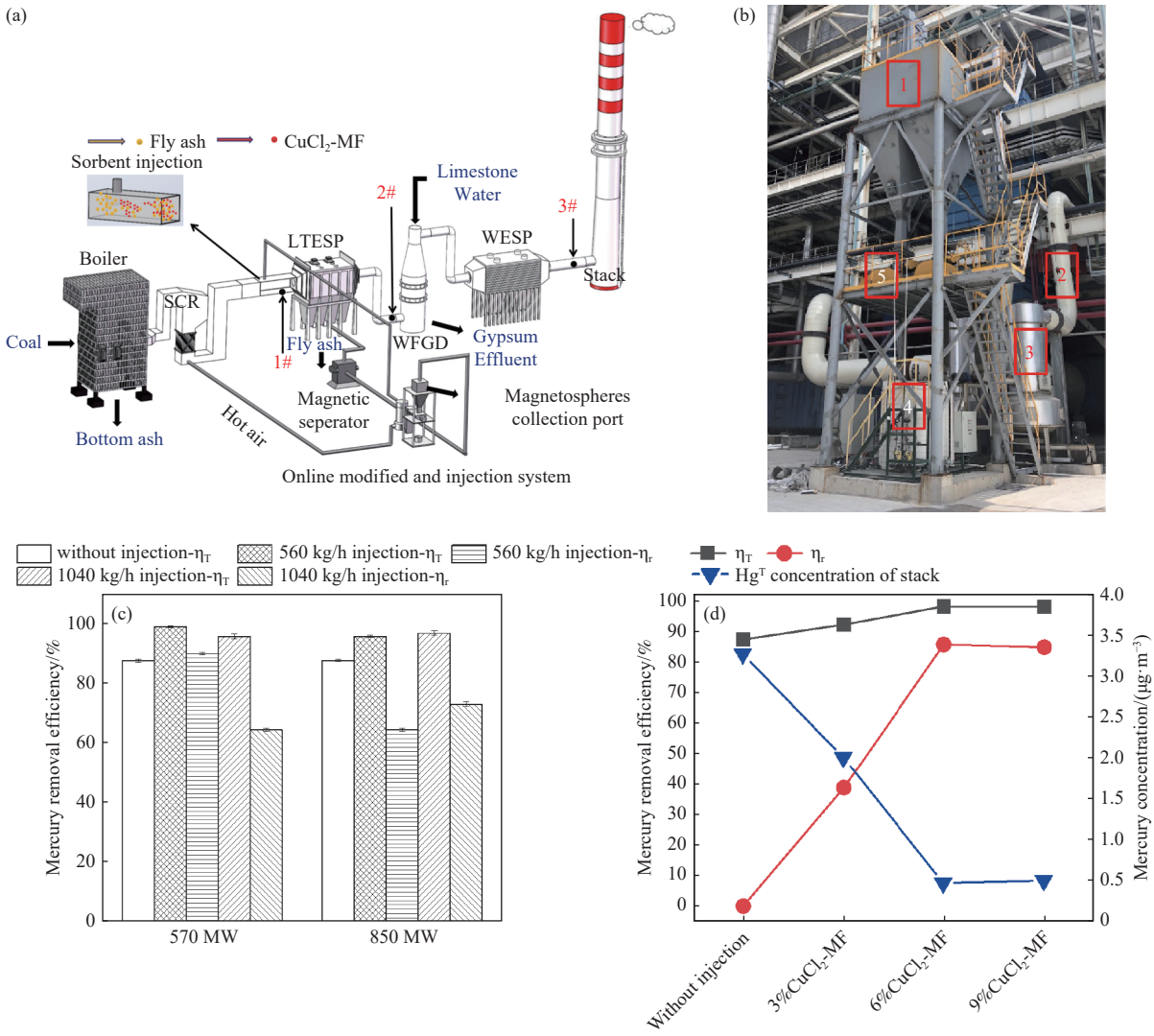



Fig. 17 On-site testing results of mercury removal with magnetospheres from the flue gas of a 1000 MW coal-fired unit: (a) Device layout diagram, (b) on-site equipment diagram (1: magnetospheres storage bin, 2: magnetospheres conveying system, 3: magnetospheres online drying device, 4: modified solution storage tank, 5: humidification and stirring equipment), (c), (d) mercury removal efficiency from flue gas with magnetospheres injection[112]
(with permission from Elsevier)

Although modified mineral and modified fly ash adsorbents have successfully achieved efficient mercury removal from coal-fired flue gas in practical applications, maintaining the flue gas mercury concentrations at low levels, from the perspective of mercury migration and transformation, the gaseous mercury in flue gas is merely transferred to the solid-phase product-fly ash. The mercury present in the fly ash poses potential risks of secondary release, and the mixing of mercury containing adsorbents may also affect the secondary utilization of fly ash. In contrast, magnetospheres mercury removal technology not only achieves highly efficient mercury removal (near zero emissions) before the dust collector but also enables the fly ash collected at the bottom of the precipitator following the mercury removal to be regenerated through magnetic separation. The regenerated and reactivated magnetic beads can be re-injected into the flue duct for subsequent mercury removal cycles, thereby effectively mitigating the risks of secondary mercury release and having great prospects for widespread application and promotion.

## 5 Resource recovery technology for mercury from multi-phase products of coal combustion

In March 2022, the Fourth Conference of the Parties to the Minamata Convention (COP4) explicitly stated that primary mercury mining will be completely phased out by 2032. As the country with the largest global demand for mercury, China will face a severe shortage of mercury resources, with the mercury market price continuing to rise. As of September 2024, the price of mercury has exceeded 1.4 million CNY/tonne[114]. Consequently, there is an urgent need to adopt high efficient recovery technologies to treat large amounts of mercury-containing waste, in order to promote the sustainable use of mercury resources. Based on

this context, the development of the third-tier mercury reduction strategy for engineering applications requires the establishment of a comprehensive technical system combining the high efficient mercury removal from flue gas with the mercury resource recovery. After mercury removal by adsorbent flue gas injection, the fly ash, gypsum, and recyclable mercury-containing magnetic beads that were originally disposed of as hazardous waste are converted into high-value mercury resources. This enables the paradigm shift from "pollution control" to "resource recycling" while ensuring the near-zero mercury emissions, thereby achieving overall optimization of environmental benefits, economic viability, and engineering feasibility. This subsection first summarizes the current mercury recovery technologies from mercury-containing waste, then proposes that future research directions should focus on the high-value-added utilization of products, and developing the integrated technologies that can simultaneously achieve high-efficiency mercury removal from flue gas and resource recovery.

### 5.1 Mercury recovery technology by pyrometallurgy

Pyrometallurgical mercury recovery processes have been extensively developed and applied. This technology uses the characteristics of mercury volatilization at high temperature to extract mercury from waste and recover liquid elemental mercury through three sequential steps of pretreatment, thermal treatment, and condensation purification. Massacci et al.[115] successfully recovered all mercury from a waste *via* thermal desorption at 500−700 °C without any pretreatment. Park and Rhee[116] determined the mercury content in the waste fluorescent lamp phosphor by pyrolysis technology, and found that the optimum conditions were 400 °C of temperature and 6 h of retorting time. To further enhance the mercury recovery efficiency, a vacuum thermal desorption method was developed. Lee et al.[117] processed a mercury-containing waste under vacuum conditions at 400 °C and 6.6 kPa pressure, achieving a mercury recovery rate of 75.23%. Liu et al.[118] utilized a microwave heating technology to reduce the activation energy for mercury desorption, reaching 99.98% of mercury removal with treatment at 500 °C for only 30 min. Nevertheless, pyrometallurgical mercury recovery technologies have certain limitations. On the one hand, impurities such as sulfur and chlorine present in waste can affect the purity of the recovered products and may lead to secondary pollution; on the other hand, this method has high energy consumption and is not suitable for processing the waste with low mercury content.

### 5.2 Mercury recovery technology by hydrometallurgy

Hydrometallurgical mercury recovery technology has become the main development direction for mercury recovery processes. The technical core of this method is to transfer mercury from solid-phase waste to the liquid phase through leaching solution, with the mercury existed in the form of ions, followed by recovery of the liquid mercury *via* electrochemical reduction or chemical precipitation. Hydrometallurgical technology has the advantages of low energy consumption and less secondary pollution. Coskun et al.[119] successfully recovered the majority of mercury through oxidative leaching hydrometallurgical extraction, employing three distinct reducing agents for the cementation. Hu et al.[120] utilized an electroleaching process to treat the waste lamp phosphor, achieving a mercury recovery rate of 99% (as illustrated in Figure 18). Ozgur et al.[121] developed an equipment system that captures mercury with nanoadsorbents and recovers mercury through electrolysis. This system utilized a magnetite nanoparticle adsorbent that could remove up to 90% of mercury vapor within 1 h and could be regenerated without losing activity, achieving a mercury vapor recovery rate of 85% within 4 h. Al-Ghoudi et al.[122] first proposed that combining microwave-assisted leaching with conventional acid leaching could double the amount of mercury leached, and microbial strains could subsequently treat the leached mercury. Bussi et al.[123] integrated sodium hypochlorite extraction with photocatalytic process, using titanium oxide as the catalyst and citric acid as the reducing agent, successfully recovering over 95% of mercury. Back et al.[124] enhanced the mercury recovery efficiency from sludge by the introduction of NaOH. In summary, the hydrometallurgical mercury recovery technology can overcome the limitations of pyrometallurgical recovery methods; however, there are several challenges to face, particularly the substantial consumption of chemical reagents during leaching and the difficulties associated with the wastewater treatment. Consequently, future research should thoroughly investigate the leaching solution selection and process flowsheet optimization for the hydrometallurgical mercury recovery technologies to satisfy the efficiency and economic requirements of industrial-scale applications.

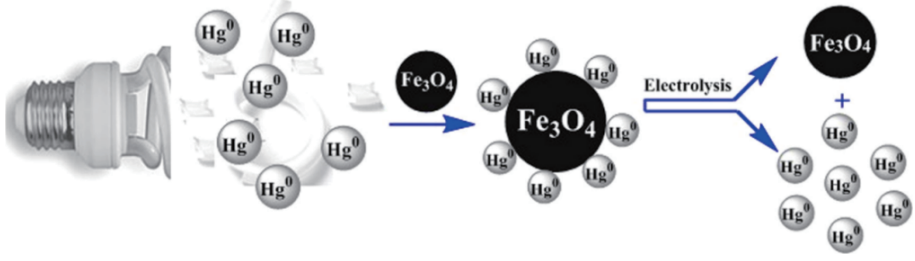



Fig. 18 Fluorescent lamp magnetic material electrocatalytic recovery of elemental mercury[120] (with permission from Elsevier)

### 5.3 Mercury high value-added utilization technology

With the increasingly severe shortage of mercury resources in China and the continuous improvement of environmental protection standards, conventional mercury recovery methods are difficult to meet the dual requirements of economic benefits and environmental protection at the same time. Therefore, how to achieve diversified waste recovery processes and high-value-added utilization of mercury has become a research priority among scholars.

Mercury and selenium exist as associated elements in certain minerals. Fu et al.[125] developed a mercury extraction method for heavy acid sludge, employing a mixed heating method of hydrochloric acid and chlorohydrochloric acid to obtain a mixed solution of mercuric chloride, followed by alkali neutralization for the selenium separation and recovery, and finally extracting high-purity mercury by vacuum rectification. Wang et al.[126] roasted an acid sludge under inert gas atmosphere, achieving the synergistic recovery of both mercury and selenium, coupled with cyanidation for the gold and silver extraction. Furthermore, the high-value transformation of mercury products is a critical direction for technological upgrading. As illustrated in Figure 19, mercury selenide (HgSe) exhibits exceptional optical properties and can serve as raw material for the high-end applications such as solar cells and mid-infrared photodetectors, possessing a considerable market value. Xiao et al.[127] proposed a method for the directional capture of mercury from flue gas using high-activity selenium, successfully synthesizing mercury selenide raw materials with excellent optical properties, which can be extended to the field of optical device development in the future.

Furthermore, as illustrated in Figure 20, Xiao et al.[128] fabricated a porous spherical carrier based on the extrusion-spheronization method, and subsequently synthesized a formed selenium-based adsorbent through nano-selenium modification for packed fixed-bed applications to achieve directional recovery of mercury from flue gas. This adsorbent had a capacity of 101.04 mg/g, substantially exceeding that of conventional adsorbents. Additionally, a process scheme for directional recovery of HgSe and the carrier regeneration using selenium-based forming adsorbents was proposed.

Based on the aforementioned approach, a HgSe high-value recovery system capable of stable operation under industrial flue gas conditions is developed (as illustrated in Figure 21(a), (b)).

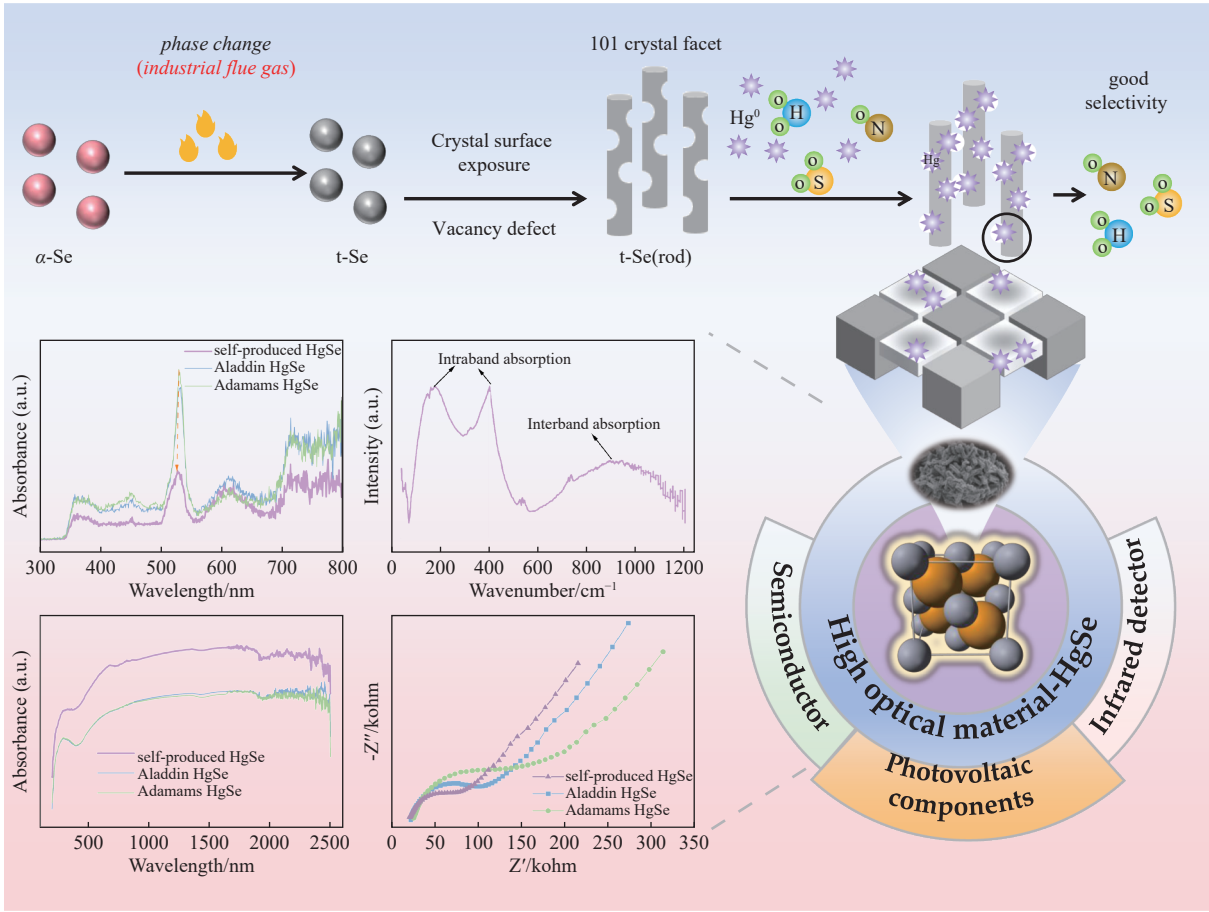



Fig. 19 Principle of mercury removal from high activity selenium (t-Se) flue gas and high value-added utilization of HgSe[127] (with permission from Wiley)

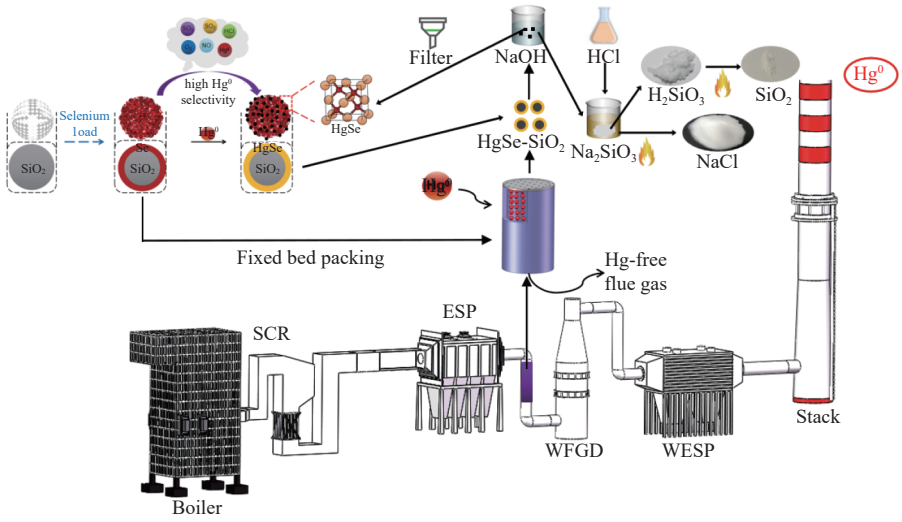



Fig. 20 Schematic diagram of flue gas mercury removal principle using selenium-loaded adsorbent ($Se/SiO_2$)[128] (with permission from Elsevier)

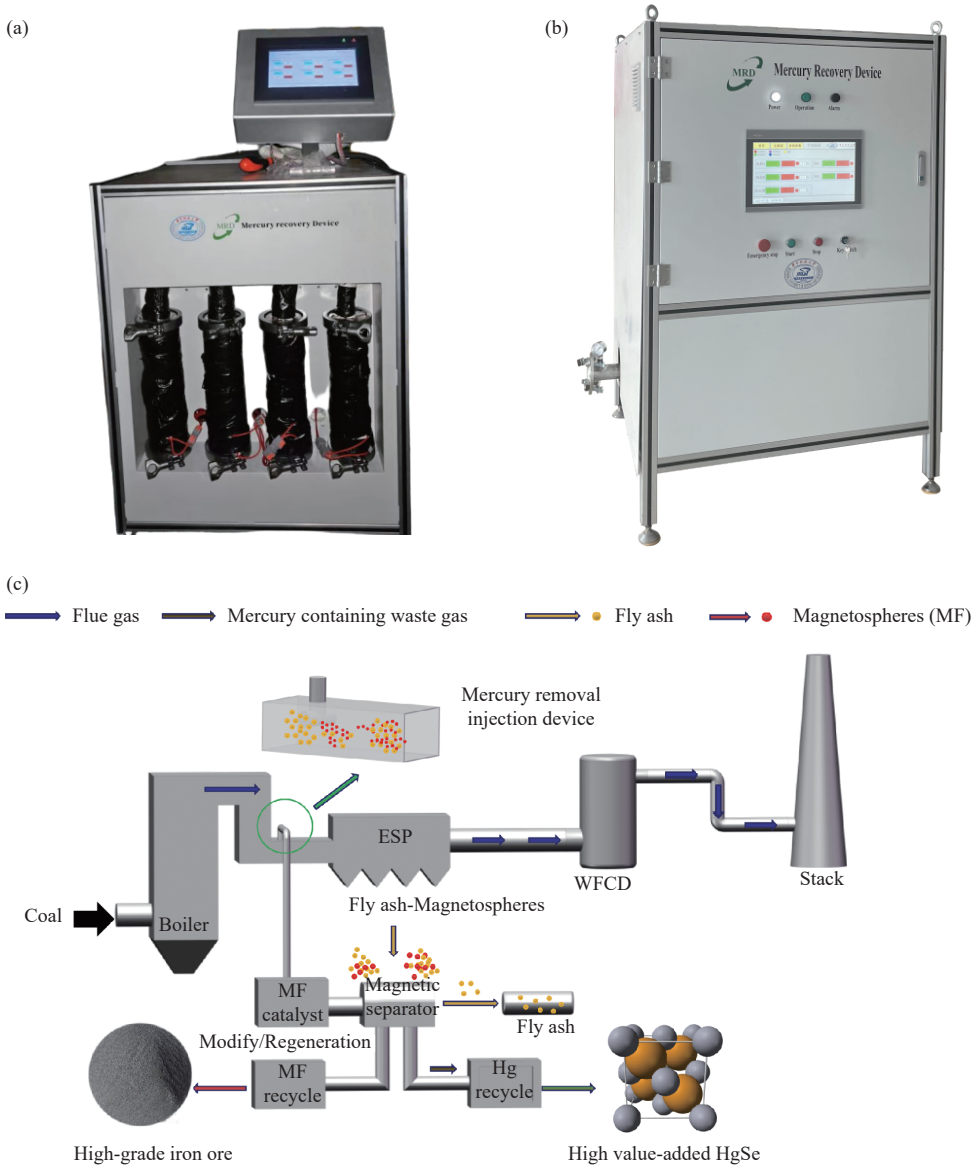



Fig. 21 Technology for magnetospheres mercury removal and mercury recovery

This system integrated with the magnetospheres mercury removal technology, in which mercury desorbed from the high-concentration mercury-laden magnetospheres surfaces entered the mercury recovery unit for directional recovery, with direct synthesis of HgSe product, ultimately forming an integrated technology combining magnetospheres mercury removal and mercury recovery (as illustrated in Figure 21(c)). Compared with the developed magnetospheres mercury removal technology, this approach not only achieves efficient mercury removal from flue gas but also successfully recovers HgSe product, preventing the mercury transformation into other products and associated secondary release risks, embodying the concept of "detoxifying with waste, transforming waste into treasure."

In the future, the mercury emission reduction in coal-fired flue gas will advance toward the integration of mercury removal and mercury recovery, as well as the high-value utilization of products, which have stringent requirements on the purification processes and high-value application technological pathways of mercury products.

## 6 Summary and Outlook

### 6.1 Summary

China's energy structure has long been dominated by coal, with the coal-based energy system remaining irreplaceable in its strategic position. Given the diverse coal types and complex combustion furnace configurations in China, there is an urgent need to develop differentiated whole-process mercury control strategies. Based on a systematic analysis of the occurrence forms of mercury in coal-fired flue gas and its migration-transformation patterns within ultra-low emission pollutant control systems, this review summarizes and compares the control technologies at different stages about the technical path and engineering feasibility, obtaining a hierarchical technical understanding. Currently, as the first tier of strategy, the synergistic mercury removal based on the existing pollutant control devices is the foundational pathway for mercury emission reduction in the coal-fired units. However, the removal effectiveness of this strategy is mainly influenced by the flue gas composition, operating parameters, and the coupling relationships between pollutant control devices. It has the advantages in controlling the particulate-bound mercury ($Hg^p$) and oxidized mercury ($Hg^{2+}$), but its removal capability for elemental mercury ($Hg^0$) is limited. To address this limitation, the second tier of strategy involves the development of adsorption and catalytic oxidation technologies, particularly the regenerable fly ash magnetic beads mercury removal technology, which has shown promising potential for enhancing the $Hg^0$ removal efficiency and possesses prospects for the engineering-scale application. Based on the first and second tier of strategies, this review prospectively proposes a third-tier mercury control strategy, namely the development of multi-phase product resource utilization technologies for coal-fired power plants, which is of significant importance for achieving the emission control of full-species mercury in coal-fired flue gas and the mercury resource high-value utilization. Among them, magnetospheres mercury removal and the HgSe recovery technology enable the enrichment and centralized recovery of mercury during flue gas treatment, fundamentally avoiding the secondary pollution while greatly reducing the system operating costs, thereby realizing the technical concept of "detoxifying with waste, transforming waste into treasure." In summary, the three-tier mercury emission reduction strategy exhibits a progressive evolution from "synergistic control" to "active removal," and subsequently to "resource utilization" in the technical objectives and implementation pathway. This not only aligns with the current mercury removal technologies in the coal-fired power plants in China, but also provides systematic technical support for meeting the requirements of the Minamata Convention and increasingly stringent mercury emission standards.

### 6.2 Outlook

With the continuous advancement of the implement of international Minamata Convention compliance requirements, mercury emissions from coal-fired flue gas in China will face the increasingly stringent standards in the future, while the resource recovery and high-value utilization of mercury will become principal development trends. Research priorities should concentrate on the following aspects:

(1) The structure-activity relationships between coal type differentiation and mercury emission characteristics should be elucidated. There are many kinds of coal and combustion furnaces in China, and there are obvious differences in mercury content, occurrence form and thermal conversion characteristics of coal in different regions. Future research should focus on revealing the influence mechanisms of coal differences on the mercury migration, release, and speciation transformation during combustion. Through big data analysis and statistical modeling, a quantitative structure-activity relationship model between coal characteristics and mercury emission behaviors should be established, which can accurately predict the mercury emission level and provide scientific basis for the coal-fired power plants to choose suitable mercury control strategies.

(2) The study on the synergistic mercury removal by conventional flue gas purification equipment under flexible peaking operation modes in the power plant should be conducted. For SCR systems, the development of the catalysts with dual functions for mercury removal and denitrification and the establishment of an efficient, recyclable catalyst regeneration system to enhance the

activity and life under low-temperature and complex operating conditions should be focused on. Simultaneously, CFD and other numerical simulation tools should be employed to optimize the catalyst layout and reactor structures, improving the gas-solid contact efficiency. For WFGD systems, because most current synergistic mercury removal research remains at laboratory scale, there is an urgent need for the demonstration studies under industrial operating conditions to identify the critical influencing factors for $Hg^0$ re-emission and propose targeted control measures.

(3) The demonstration and application of a near-zero emission technology for all forms of mercury should be enhanced. At present, the mercury removal technology with adsorbents is mostly focused on the laboratory research, with significant disconnect from engineering applications. Current adsorbent mercury removal technologies are predominantly concentrated on the laboratory research. Therefore, future efforts should be made on the field demonstration and applications of adsorbents/catalysts. On the one hand, a prediction model for the mercury removal efficiency of adsorbents should be built, the structure of injection devices by using simulation software such as Fluent should be optimized, and the pilot-scale mercury removal trials should be carried out to realize the directional design and engineering optimization of adsorbents; on the other hand, *via* the strengthening of demonstration and promotion of the mercury removal and mercury recovery technologies with magnetic beads, the technology with low-cost, high efficient and universal application will be finally formed.

(4) The directions for resource recovery and high-value utilization of mercury should be expanded. With the Minamata Convention explicitly prohibiting the mining of primary mercury mines from 2032, the demand for mercury resource recovery is increasingly urgent. Conventional pyrometallurgical recovery suffers from high energy consumption and high risk of secondary pollution, while the hydrometallurgical recovery faces the environmental pressures from wastewater treatment. Future research should first explore the efficient and economical mercury recovery process for the multi-source byproducts in the coal-fired power plants. Second, consideration should be given to the high-value transformation of recovered mercury into the high value-added products such as electronic materials or other chemicals. Finally, addressing the issue of secondary products including wastewater and residues from mercury recovery processes to minimize the environmental pollution is one of the key tasks for the future technological development.

## Declaration of Competing Interest

The authors declare no conflict of interest.

## References


[1] NATIONAL BUREAU OF STATISTICS OF CHINA. China Statistical Yearbook 2024[M]. Beijing: China Statistics Press, 2024.

[2] INTERNATIONAL ENERGY AGENCY. Coal 2024: Analysis and Forecast to 2027[R]. Paris: IEA Publications, 2024. https://www.iea.org/reports/coal-2024.

[3] UN ENVIRONMENT PROGRAMME. Global Mercury Assessment 2018[R]. Geneva: UN Environment Programme, Chemicals and Health Branch, 2019.

[4] WANG S, BAI X, SONG C, et al. Study on emission standards for atmospheric mercury and other trace elements from coal-fired power plants[J]. China Environ Sci, 2021, 41(4): 1949−1958.

[5] MINISTRY OF ECOLOGY AND ENVIRONMENT OF THE PEOPLE'S REPUBLIC OF CHINA. Environmental Protection Tax Law of the People's Republic of China[S]. Beijing, 2025.

[6] UNITED NATIONS ENVIRONMENT PROGRAMME. Progress report on activities[C]//Minamata Convention on Mercury COP6. Geneva: UNEP, 2025. https://minamataconvention.org/en/meetings/cop6.

[7] HE S. Experimental and mechanistic study on catalytic oxidation of mercury in coal-fired flue gas[D]. Hangzhou: Zhejiang University, 2009.

[8] LIU Y, ZHENG C, CHENG J, et al. Forms of mercury in coal-fired flue gas and its analytical methods[J]. J Fuel Chem Technol, 2000, 28(5): 463−467.

[9] ZHANG J. Study on enrichment patterns of potential toxic trace elements and their pollution inhibition in coal[D]. Beijing: China University of Mining and Technology, 1999.

[10] FINKELMAN R. Model of occurrence of trace elements in coal[J]. US Geological Survey Open-File Report, 1981, 81: 99−322.

[11] LIU J, LU X, GUO X. Speciation analysis of trace elements arsenic and mercury in coal[J]. Huazhong Univ Sci Technol, 2000, 28(7): 71−73.

[12] LIU Y. Migration and transformation behavior of trace elements during coal combustion[D]. Wuhan: Huazhong University of Science and Technology, 2002.

[13] ZHENG C. Mercury Emissions and Control During Coal Combustion[M]. Beijing: Chemical Industry Press, 2010.

[14] ZHAO S, DUAN Y, WANG C, et al. Migration behavior of trace elements at a coal-fired power plant with different boiler loads[J]. Energy Fuels, 2018, 31(1): 747−754.

[15] KEVIN C, CHRISTOPHER J. Mercury transformations in coal combustion flue gas[J]. Fuel Process Technol, 2000, 65: 289−310.

[16] PAVLISH J, SONDREAL E, MANN M, et al. Status review of mercury control options for coal-fired power plants[J]. Fuel Process Technol, 2003, 82: 89−165.

[17] HALL B, SCHAGER P, LINDQVIST O. Chemical reaction of mercury in combustion flue gases[J]. Water Air

Soil Pollut, 1991, 56(1): 3−14.

[18] NIKSA S, NAIK C, BERRY M, et al. Interpreting enhanced Hg oxidation with Br addition at Plant Miller[J]. Fuel Process Technol, 2009, 90: 1372−1377.

[19] NORTON G, YANG H, BROWN B, et al. Heterogeneous oxidation of mercury in simulated post combustion conditions[J]. Fuel, 2017, 36: 107−116.

[20] ESWARAN S, STENGER H. Understanding mercury conversion in selective catalytic reduction (SCR) catalysts[J]. Energy Fuels, 2005, 19(9): 2328−2334.

[21] ESWARAN S, STENGER H. Effect of halogens on mercury conversion in SCR catalysts[J]. Fuel Process Technol, 2008, 89(11): 1153−1159.

[22] PRESTO A, GRANITE E. Survey of catalysts for oxidation of mercury in flue gas[J]. Environ Sci Technol, 2006, 40(18): 5601−5609.

[23] LI H, LI Y, WU C, et al. Oxidation and capture of elemental mercury over Si–$TiO_2$–$V_2O_5$ catalysts in simulated low-rank coal combustion flue gas[J]. Chem Eng J, 2011, 169(1-3): 186−193.

[24] PRECIADO I, YOUNG T, SILCOX G. Mercury oxidation by halogens under air- and oxygen-fired conditions[J]. Energy Fuels, 2014, 28(2): 1255−1261.

[25] ZHOU Z, LIU X, ZHAO B, et al. Effects of existing energy-saving and air pollution control devices on mercury removal in coal-fired power plants[J]. Fuel Process Technol, 2015, 131: 99−108.

[26] YANG J, ZHAO Y, ZHANG J, et al. Research progress on capture and oxidation of mercury by fly ash from coal-fired power plants[J]. J Power Eng, 2014, 34(5): 1−9.

[27] FTHENAKIS V, LIPFERT F, MOSKOWITZ P, et al. An assessment of mercury emissions and health risks from a coal-fired power plant[J]. J Hazard Mater, 1995, 44(2): 267−283.

[28] ZHANG Y, YANG J, YU X, et al. Migration and emission characteristics of mercury in coal-fired power plants of China with ultra-low emission air pollution control devices[J]. Fuel Process Technol, 2017, 158: 272−280.

[29] ZHAO S, DUAN Y, CHEN L, et al. Study on emission of hazardous trace elements in a 350 MW coal-fired power plant. Part 1: Mercury[J]. Environ Pollut, 2017, 229: 863−870.

[30] PUDASAINEE D, KIM J, YOON Y, et al. Oxidation, reemission and mass distribution of mercury in bituminous coal-fired power plants with SCR, CS-ESP and wet FGD[J]. Fuel, 2012, 93(1): 312−318.

[31] JAMES D, KILGROE D, CHARLES B, et al. Control of mercury emissions from coal-fired electric utility boilers: Interim report[R]. Virginia: National Risk Management Research Laboratory, 2002.

[32] GAO T, XIAO R, CHUAI X, et al. Study on mercury emission characteristics of large-scale circulating fluidized bed boilers and pulverized coal boilers[J]. J Fuel Chem Technol, 2022, 50(3): 275−282.

[33] XIN F, WEI S, ZHANG J, et al. Research progress on non-carbon-based sorbents for mercury removal from coal-fired flue gas[J]. J Fuel Chem Technol, 2020, 48(12): 1409−1420.

[34] BAO J, YIN H, YANG L, et al. Study on mercury removal performance of wet flue gas desulfurization systems[J]. J Power Eng, 2009, 29(7): 664−670.

[35] YANG H, LIU K, CAO Y, et al. Experimental study on mercury removal characteristics of desulfurization devices in power plant flue gas[J]. J Power Eng, 2006, 26(4): 554−557, 567.

[36] LI Z, DUAN Y, WANG Y, et al. Characteristics of mercury removal by ESP and WFGD in a 300 MW coal-fired power plant[J]. J Fuel Chem Technol, 2013, 41(4): 491−498.

[37] VAN LOON L, MADER E, SCOTT S. Sulfite stabilization and reduction of the aqueous mercuric ion: Kinetic determination of sequential formation constants[J]. J Phys Chem A, 2001, 105(13): 3190−3195.

[38] LI B. Study on catalyst design and reaction mechanism for synergistic control of nitrogen oxides and mercury[D]. Taiyuan: Taiyuan University of Technology, 2024.

[39] ZHOU T. Study on influencing factors of divalent mercury reduction in calcium-based wet flue gas desulfurization slurry[D]. Xiangtan: Xiangtan University, 2015.

[40] ZHAO L, LI C, ZHANG X, et al. Oxidation of elemental mercury by modified spent $TiO_2$-based SCR-DeNOx catalysts in simulated coal-fired flue gas[J]. Environ Sci Pollut Res, 2016, 23(2): 1471−1481.

[41] LI M. Numerical study on synergistic removal of mercury and particulate matter in electrostatic precipitator[D]. Beijing: North China Electric Power University, 2016.

[42] Fang P, Cen C, Tang Z. Experimental study on the oxidative absorption of Hg by $KMnO_4$ solution[J]. Chem Eng J, 2012, 198–199: 95–102.

[43] OMINE N, ROMERO C, KIKKAWA H, et al. Study of elemental mercury re-emission in a simulated wet scrubber[J]. Fuel, 2012, 91(1): 93−101.

[44] WU C, CAO Y, HE C, et al. Study of elemental mercury re-emission through a lab-scale simulated scrubber[J]. Fuel, 2010, 89(8): 2072−2080.

[45] TANG T, XU J, LU R, et al. Enhanced $Hg^{2+}$ removal and $Hg^0$ re-emission control from wet fuel gas desulfurization liquors with additives[J]. Fuel, 2010, 89(12): 3613−3617.

[46] OCHOA-GONZALEZ R, DIAZ SOMOANO M, MARTINEZ TARAZONA M R. Control of $Hg^0$ re-emission from gypsum slurries by means of additives in typical wet scrubber conditions[J]. Fuel, 2013, 105: 112−118.

[47] ZHANG H, LIANG D, LI L, et al. Research progress on preparation and modification of activated carbon for mercury removal from flue gas[J]. Coal Sci Technol, 2013, 41(12): 120−124.

[48] WANG F, TAN S, CAO Y, et al. Experimental study on the influence of surface characteristics of activated carbon on mercury removal in flue gas[J]. Energy Fuels, 2020, 34: 6168−6177.

[49] WANG J, ZHANG Y, ZHANG Y, et al. Influence of injection position and temperature on mercury removal by activated carbon adsorption in ultra-low emission coal-fired power plants[J]. Proc CSEE, 2019, 39(11): 3303−3312.

[50] ZHOU Q, DUAN Y, CHEN M, et al. Studies on mercury adsorption species and equilibrium on activated carbon surface[J]. Energy Fuels, 2017, 31(12): 14211−14218.

[51] LIU Z, ADEWUYI Y, SHI S, et al. Removal of gaseous $Hg^0$ using novel seaweed biomass-based activated carbon[J]. Chem Eng J, 2019, 366: 41−49.

[52] SHI Q, WANG Y, ZHANG X, et al. Hierarchically porous biochar synthesized with $CaCO_3$ template for efficient $Hg^0$ adsorption from flue gas[J]. Fuel Process Technol, 2020, 199: 106247.

[53] LIN G, PENNER J, CLACK H, et al. Radiative forcing associated with particulate carbon emissions resulting from the use of mercury control technology[J]. Environ Sci Technol, 2014, 48: 10519−10523.

[54] LIU Y, BISSON T, YANG H, et al. Recent developments in novel sorbents for flue gas clean-up[J]. Fuel Process Technol, 2010, 91(10): 1175−1197.

[55] WU D, ZHANG S, ZHU T. Controlling mercury emission for China's coal-fired electricity plants: An economic analysis[J]. Energy Procedia, 2011, 5: 1439−1454.

[56] ANCORA M, ZHANG L, WANG S, et al. Economic analysis of atmospheric mercury emission control for coal-fired power plants in China[J]. J Environ Sci, 2015, 33: 125−134.

[57] DU W, YIN L, ZHUO Y, et al. Experimental study on mercury removal by non-carbon-based sorbent injection in a 100 MW coal-fired power plant[J]. J Chem Ind Eng, 2014, 65(11): 4413−4419.

[58] DU W, YIN L, ZHUO Y, et al. Study on mercury removal by non-carbon-based sorbents modified with transition metal halides[J]. J Eng Thermophys, 2011, 32(7): 1236−1240.

[59] AKHMETOV D, ANISKIN A, APSHIKUR B, et al. Effect of electrochemically activated mixing water on strength and pore structure of fly-ash autoclaved aerated concrete[J]. Sustain Chem Pharm, 2025, 44: 101981.

[60] YAO Z, JI X, SARKER P, et al. A comprehensive review on the applications of coal fly ash[J]. Earth-Sci Rev, 2015, 141: 105−121.

[61] YU J, JIN D, GUO Z, et al. Effects of temperature and modification concentration on mercury adsorption performance of modified fly ash[J]. J Therm Power Eng, 2021, 36(11): 94−96.

[62] DENG S, SHU Y, LI S, et al. Chemical forms of fluorine, chlorine, oxygen and carbon in coal fly ash and their correlations with mercury retention[J]. J Hazard Mater, 2016, 301: 400−406.

[63] ZHANG Y, ZHANG Z, LIU Z, et al. Study on the mercury captured by mechanochemical and bromide surface modification of coal fly ash[J]. Fuel, 2017, 200: 427−434.

[64] RIM I, HEZIL N, FELLAH M, et al. Surfactants modification of kaolin for enhanced mercury adsorption[J]. J Water Process Eng, 2025, 76: 108201.

[65] LIU H. Study on mercury removal and reaction mechanism by modified mineral adsorbents[D]. Wuhan: Huazhong University of Science and Technology, 2020.

[66] CAI J, SHEN B, LI Z, et al. Removal of elemental mercury by clays impregnated with KI and KBr[J]. Chem Eng J, 2014, 241: 19−27.

[67] SHEN B, CHEN J, YUE S. Removal of elemental mercury by titanium-pillared clay impregnated with potassium iodide[J]. Microporous Mesoporous Mater, 2015, 203: 216−223.

[68] LIU H, YANG J, TIAN C, et al. Mercury removal from coal combustion flue gas by modified palygorskite adsorbents[J]. Appl Clay Sci, 2017, 147: 36−43.

[69] YU M, DONG Y, WANG P, et al. Research progress on the influence of chlorine element on mercury removal from coal-fired flue gas[J]. Chem Ind Eng Prog, 2012, 31: 1610−1614.

[70] LYU X, WANG J, GUO Y, et al. Simultaneous removal of elemental mercury and hydrogen sulfide from coal gas by composite metal oxide adsorbents[J]. Chem Ind Eng Prog, 2011, 30(S1): 79−83.

[71] LI N, WEI H, DUAN Y, et al. Research progress on renewable mercury removal adsorbents[J]. Power Gener Equip, 2019, 33(1): 28−32.

[72] HU P, DUAN Y, CHEN Y, et al. Synergistic denitrification and mercury removal characteristics of Mo–Mn/$TiO_2$ catalysts[J]. China Environ Sci, 2018, 38(2): 523−531.

[73] ZHANG Z, WU J, LI B, et al. Removal of elemental mercury from simulated flue gas by ZSM-5 modified with Mn–Fe mixed oxides[J]. Chem Eng J, 2019, 375: 121946.

[74] YANG J, ZHANG M, LI H, et al. Simultaneous NO reduction and $Hg^0$ oxidation over $La_{0.8}Ce_{0.2}MnO_3$ perovskite catalysts at low temperature[J]. Ind Eng Chem Res, 2018, 57: 9374−9385.

[75] DONG L, HUANG Y, YUAN Q, et al. Experimental study on mercury removal from flue gas over Mn-loaded Ti–Zr and Ti–Sn composite oxide catalysts[J]. J Fuel Chem Technol, 2020, 48(6): 741−751.

[76] WANG T, YANG Y, WANG J, et al. Preadsorbed $SO_3$ inhibits oxygen atom activity for mercury adsorption on Cu/Mn doped $CeO_2$(110) surface[J]. Energy Fuels, 2020, 34: 4734−4744.

[77] ZHU M, YAN Q, DUAN Y, et al. Study on preparation and mercury adsorption characteristics of columnar sulfur-impregnated activated petroleum coke[J]. Energy Fuels, 2020, 34: 10740−10751.

[78] MILLER S, DUNHAM G, OLSON E, et al. Flue gas effects on a carbon-based mercury sorbent[J]. Chem Eng J, 2000, 65–66: 343–363.

[79] WANG Y, CHEN Z, YAN Q, et al. Evaluation and application of silver-loaded molecular sieves for renewable mercury removal from natural gas[J]. Petrol Nat Gas Chem Ind, 2021, 50(4): 1−7.

[80] ZHOU Z, CAO T, LIU X, et al. Mechanistic investigation of elemental mercury adsorption over silver-modified vanadium silicate: A DFT study[J]. J Hazard Mater, 2021, 404: 124108.

[81] XIE Y, YAN B, TIAN C, et al. Efficient removal of elemental mercury ($Hg^0$) by SBA-15-Ag adsorbents[J]. J Mater Chem A, 2014, 2(42): 17730−17734.

[82] LUO G, YAO H, XU M, et al. Carbon nanotube-silver composite for mercury capture and analysis[J]. Energy Fuels, 2010, 24(1): 419−426.

[83] YANG J, CHEN H, QIAO F, et al. Engineering single-atom Pd sites in ZIF-derived porous $Co_3O_4$ for enhanced elementary mercury removal[J]. Sep Purif Technol, 2022, 309: 123050.

[84] LIU D, LI B, WU J, et al. Elemental mercury capture from industrial gas emissions using sulfides and selenides: A review[J]. Environ Chem Lett, 2021, 19: 1395−1411.

[85] XIAO Y, LIU Q, HUANG Y, et al. Coordinative sulfur site over flower-structured $MoS_2$ for efficient elemental mercury uptake from coal-fired flue gas[J]. Chem Eng J, 2022, 434: 134649.

[86] LIU H, RUAN W, ZHANG Z, et al. Dual 2-dimensional CuSe/g-$C_3N_4$ nano-heterostructure for boosting immobilization of elemental mercury in flue gas[J]. Chem Eng J, 2022, 435: 134696.

[87] XIAO R, ZHANG Y, LONG K, et al. Multiscale investigation of 3D morphology $SnSe_2$ for mercury removal from flue gas: Experimental and simulation studies[J]. Energy Fuels, 2024, 38: 16610−16621.

[88] LI H, MENG F, ZHU P, et al. Biomimetic mercury immobilization by selenium functionalized polyphenylene sulfide fabric[J]. Nat Commun, 2024, 15(1): 1292.

[89] LONG K, XIAO R, ZHANG T, et al. Efficient gaseous mercury removal by nano-amorphous red selenium and recycling design of HgSe nanoparticles[J]. Chem Eng J, 2024, 153190.

[90] WANG L, LI Y, SUN R, et al. Experimental and theoretical study on recovered nano amorphous selenium as efficient adsorbents for mercury capture from flue gas[J]. J Clean Prod, 2024, 450: 141804.

[91] ZHANG Y, YANG J, ZHAO Y, et al. Performance and process-route study of recyclable magnetic-bead removal of elemental mercury from coal-fired flue gas[J]. Therm Power Gener, 2016, 45(10): 10−15.

[92] ZHANG X, SHEN B, ZHANG X, et al. Study on Mn-loaded Fe-based MOFs mercury removal agent for flue-gas mercury removal[J]. J Fuel Chem Technol, 2019, 47(1): 113−120.

[93] ZHONG C, WANG H, WU A, et al. Study on the activity effect of full tailings paste filling with fly ash[J]. Met Mine, 2017, (2): 184−187.

[94] VASSILEV S, MENENDEZ R, BORREGO A, et al. Phase-mineral and chemical composition of coal fly ashes as a basis for their multicomponent utilization. 3. Characterization of magnetic and char concentrates[J]. Fuel, 2004, 83: 1563−1583.

[95] CHEN Y, FENG Q. Biomagnetic-bead mercury removal: A new approach for coal-fired and metallurgical flue-gas treatment[J]. J Environ Eng, 2020, 14(1): 1−2.

[96] GU Y, WANG S. Research progress on the mechanism of mercury adsorption and oxidation by modified coal fly ash[J]. Chem Ind Eng Prog, 2017, 36(11): 4257−4264.

[97] DANG L. Removal of elemental mercury from simulated flue gas using Cu-Fe modified magnetic beads[D]. Dalian: Dalian University of Technology, 2021.

[98] YANG J, ZHAO Y, ZHANG S, et al. Mercury removal from flue gas by magnetospheres present in fly ash: Role of iron species and modification by HF[J]. Fuel Process Technol, 2017, 167: 263−270.

[99] WANG S, ZHANG L, LI G, et al. Mercury emission and speciation of coal-fired power plants in China[J]. Atmos Chem Phys, 2010, 10: 1183−1192.

[100] YANG J, ZHAO Y, ZHANG J, et al. Removal of elemental mercury from flue gas by recyclable $CuCl_2$-modified magnetospheres catalyst from fly ash. Part 1. Catalyst characterization and performance evaluation[J]. Fuel, 2016, 164: 419−428.

[101] YANG J, ZHAO Y, ZHANG J, et al. Removal of elemental mercury from flue gas by recyclable $CuCl_2$-modified magnetospheres catalyst from fly ash. Part 2. Identification of involved reaction mechanism[J]. Fuel, 2016, 167: 366−374.

[102] YANG J, ZHAO Y, ZHANG J, et al. Removal of elemental mercury from flue gas by recyclable $CuCl_2$-modified magnetospheres catalyst from fly ash. Part 3. Regeneration performance in realistic flue gas atmosphere[J]. Fuel, 2016, 173: 1−7.

[103] CHEN S, HSI H, NIAN S, et al. Synthesis of N-doped $TiO_2$ photocatalyst for low-concentration elemental mercury removal under various gas conditions[J]. Appl Catal B: Environ, 2014, 160: 558−565.

[104] FENG D, XU S, LIU G. Application of immobilized $TiO_2$ photocatalysis to improve the inactivation of Heterosigma akashiwo in ballast water by intense pulsed light[J]. Chemosphere, 2015, 125: 102−107.

[105] ZHOU X. Preparation of $MO_x/TiO_2$ composite materials and experimental study on their photocatalytic mercury removal[D]. Shanghai: Shanghai Electric Power University, 2018.

[106] SILVA A, SILVA C, DRAŽIĆ G, et al. Ce-doped $TiO_2$ for photocatalytic degradation of chlorophenol[J]. Catal Today, 2009, 144: 13–18.

[107] ZHANG Y, ZHAO Y, XIONG Z, et al. Elemental mercury removal by $I^-$-doped $Bi_2WO_6$ with remarkable visible-light-driven photocatalytic oxidation[J]. Appl Catal B: Environ, 2021, 282: 119534.

[108] LIU H, GAO T, YANG G. Elemental mercury removal from flue gas using modified tonstein: Performance of adsorbent injection at an entrained flow reactor system and 50-MW coal-fired power plant in China[J]. J Clean Prod,

2021, 287: 124998.
[109] ZHANG Y, MEI D, WANG T, et al. In-situ capture of mercury in coal-fired power plants using high surface energy fly ash[J]. Environ Sci Technol, 2019, 53: 7913−7920.
[110] YANG J, ZHAO Y, GUO X, et al. Removal of elemental mercury from flue gas by recyclable $CuCl_2$-modified magnetospheres from fly ash. Part 4. Performance of sorbent injection in an entrained flow reactor system[J]. Fuel, 2018, 220: 403−411.
[111] ZHOU Y, YANG J, DONG L, et al. Removal of elemental mercury from flue gas by recyclable $CuCl_2$-modified magnetospheres from fly ash: Part 5. Industrial scale studies at a 50 $MW_{th}$ coal-fired power plant[J]. Fuel, 2020, 266: 117052.
[112] XIAO R, GAO T, CUI X, et al. Removal of elemental mercury from flue gas by recyclable $CuCl_2$-modified magnetospheres from fly ash: Part 6. Commercial scale demonstration at a 1000 $MW_{th}$ coal-fired power plant[J]. Fuel, 2021, 266: 117052.
[113] XIAO R, ZHANG Y, WEI S, et al. Swirl diffusion strategy boosts mercury removal effectiveness of magnetospheres injector[J]. Chem Eng J, 2024, 481: 148582.
[114] CHAI L, LIU H, WU J, et al. Progress in mercury pollution control and resource recovery technologies in non-ferrous metallurgy[J]. Nonferrous Met, 2024: 51–61.
[115] MASSACCI P, PIGA L, FERRINI M. Applications of physical and thermal treatment for the removal of mercury from contaminated materials[J]. Miner Eng, 2000, 13(8/9): 963−967.
[116] PARK H, RHEE S. Estimation of retorted phosphor powder from spent fluorescent lamps by thermal process[J]. Waste Manage, 2016, 50: 257−263.
[117] LEE W, EOM Y, LEE T. Mercury recovery from mercury-containing wastes using a vacuum thermal desorption system[J]. Waste Manage, 2017, 60: 546−551.
[118] LIU C, PENG J, LIU J, et al. Catalytic removal of mercury from waste carbonaceous catalyst by microwave heating[J]. J Hazard Mater, 2018, 358: 198−206.
[119] COSKUN S, CIVELEKOGLU G. Recovery of mercury from spent fluorescent lamps via oxidative leaching and cementation[J]. Water Air Soil Pollut, 2015, 226: 1−13.
[120] HU Z, KURIEN U, MURWIRA K, et al. Development of a Green Technology for Mercury Recycling from Spent Compact Fluorescent Lamps Using Iron Oxides Nanoparticles and Electrochemistry[J]. ACS Sustainable Chem Eng, 2016, 4(4): 2150−2157.
[121] OZGUR C, COSKUN S, AKCIL A, et al. Combined oxidative leaching and electrowinning process for mercury recovery from spent fluorescent lamps[J]. Waste Manage, 2016, 57: 215−219.
[122] AL-GHOUDI M, ABUQAOUD R, ABU-DIEYEH M. Detoxification of mercury pollutant leached from spent fluorescent lamps using bacterial strains[J]. Waste Manage, 2016, 49: 238−244.
[123] BUSSI J, CABRERA M, CHIAZZARO J, et al. The recovery and recycling of mercury from fluorescent lamps using photocatalytic techniques[J]. J Chem Technol Biotechnol, 2010, 85(4): 478−484.
[124] BACK S, LEE E, SEO Y, et al. The effect of NaOH for the recovery of elemental mercury from simulated mixture wastes and waste sludge from an industrial process using a thermal desorption process[J]. J Hazard Mater, 2020, 384: 121291.
[125] FU G, ZHAO Z, HUANG S. Extraction method of mercury from heavy acid mud: CN201710211864.1[P]. 2017-06-27.
[126] WANG M, MA J, MA C. A method for recovering selenium, mercury, gold and silver from acid mud: CN201510259346.8[P]. 2015-07-29.
[127] XIAO R, YANG J, ZHANG Y, et al. Efficient and selective immobilization and direct conversion of mercury into optical material-HgSe via highly active trigonal phase selenium (t-Se)[J]. Adv Funct Mater, 2025, 35(32): 202500134.
[128] XIAO R, ZHANG Y, WEI S, et al. A high efficiency and high capacity mercury adsorbent based on elemental selenium loaded $SiO_2$ and its application in coal-fired flue gas[J]. Chem Eng J, 2022, 453: 139946.

# 中国燃煤烟气汞排放控制策略

肖日宏，罗长新，吴煜梓，汤承睿，熊　卓，张军营，赵永椿*

（华中科技大学 能源与功力工程学院 煤燃烧与低碳利用全国重点实验室, 湖北 武汉 430074）

**摘　要：**燃煤过程中排放的汞具有高毒性、易挥发性和生物富集性，长期威胁生态系统和人类健康。本工作综述了中国燃煤汞排放现状及控制政策，分析了煤燃烧过程中汞的分布特性和迁移转化规律，重点总结了超低排放改造后，污染物控制装置在协同脱汞方面的机理及效果。基于此，构建了“协同增效-深度净化-资源循环”的递进式燃煤烟气汞减排策略：第一层次，通过优化污染物控制系统的运行参数，提升各控制装置的协同脱汞效率；第二层次，研发高效的燃煤烟气汞吸附和催化氧化技术，重点发展可工业化应用的脱汞技术；第三层次，开发燃煤电厂高效脱汞和汞回收一体化技术（如磁珠脱汞及汞回收技术），聚焦于汞高附加值利用。结合最新的国际履约形势和中国环境税法政策，指出未来中国燃煤烟气汞排放控制的研发方向，为中国国际履约和燃煤烟气污染物近零排放提供理论与技术支撑。

**关键词：**煤燃烧；汞；吸附/催化；汞回收；减排策略

**中图分类号**：X511　　**文献标识码**：A

**作者简介**：



肖日宏(1998)，博士研究生，研究方向为燃煤污染物汞减排及资源回收，d202380511@hust.edu.cn。



赵永椿(1982)，教授，博士生导师，主要从事研究方向为燃煤减污降碳技术研发及产物资源化利用，yczhao@hust.edu.cn。